WATER SCIENCE SERIES

Mapping the Snow Sensitive Zone in the Upper Columbia River Basin, Canada

Natasha Neumann

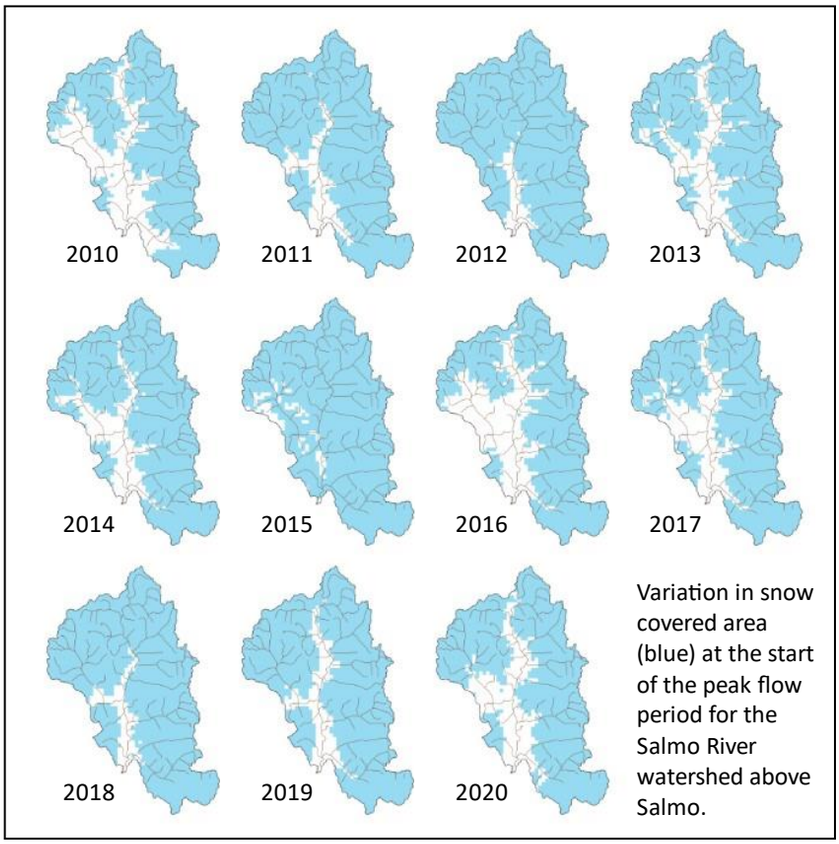

Variation in snow covered area (blue) at the start of the peak flow period for the Salmo River watershed above Salmo.

November 2023

BRITISH COLUMBIA

No. 2023-07

The **Water Science Series** are scientific technical reports relating to the understanding and management of B.C.'s water resources. The series communicates scientific knowledge gained through water science programs across B.C. government, as well as scientific partners working in collaboration with provincial staff. For additional information visit: http://www2.gov.bc.ca/gov/content/environment/air-land-water/water/water-science-data/water-science-series.

ISBN: 978-1-0399-0038-7

Citation:
Neumann, Natasha. 2023. Mapping the snow sensitive zone in the upper Columbia River basin, Canada. Water Science Series, WSS2023-07. Prov. B.C., Victoria B.C.

Author's Affiliation:
Natasha Neumann, PhD PAg*
B.C. Ministry of Forests, Kootenay Boundary Region
401-333 Victoria St., Nelson, B.C. V1L 4K3

*Adjunct Professor, Department of Earth, Environmental and Geographic Sciences
University of British Columbia Okanagan
1177 Research Road, Kelowna, B.C. V1V 1V7

Cover Image:
N. Neumann

Acknowledgements

This work was funded by the research program of the B.C. Ministry of Forests. GIS analysis was completed by Vicky Young (B.C. Ministry of Water, Land and Resource Stewardship) and TerraNiche Environmental Solutions. The author would like to thank Peter Ott, Senior Biometrician with Ministry of Forests, for help with the statistical analysis, as well as Robin Pike and Chris Williams for their thoughtful comments.

EXECUTIVE SUMMARY

Natural and anthropogenic forest disturbance alters snow accumulation and melt processes in forested watersheds, often resulting in greater snow accumulation and faster snowmelt in unforested areas relative to adjacent forested stands (Teti 2003; Winkler et al. 2004; Jost et al. 2007; Varhola et al. 2010; Boon 2012; Winkler et al. 2015). This may increase the potential for snowmelt synchronization across previously de-synchronized areas of a watershed and any subsequent increased peak flows may need to be considered in forestry operations planning and cumulative effects analysis. In the British Columbia interior, the H60 elevation (i.e., the elevation above which 60% of the watershed area lies) is often used as an estimate of the snow sensitive zone (SSZ, the area contributing snow meltwater during the peak flow period) (B.C. Ministry of Forests 2001). Historically, the H60 was assumed to be a conservative estimate of the SSZ, based on early work done in Colorado by Gartska et al. (1958). More recently, the increased availability of spatial snow products has created the opportunity to assess the SSZ at a broader scale than in the past (Gluns 2001; Smith et al. 2008; Neumann 2022), allowing for testing of the H60 concept.

Neumann (2022) describes a method for mapping the SSZ in the Kettle River basin using hydrometric data and a gridded snow water equivalent product available for southern B.C. from the U.S. National Operational Hydrologic Remote Sensing Center (NOHRSC 2004). In this study, the same methods were used to map the SSZ for 57 gauged watersheds across the upper Columbia River basin in Canada. Watersheds were grouped by general physiographic region to reflect expected differences in the factors controlling snow accumulation and melt, with 15 in the western plateau region and 42 in the eastern mountainous region. For each watershed, SSZ lower limit elevations were determined using both the median ($Elev_{median\ SCA}$) and maximum ($Elev_{max\ SCA}$) snow covered areas (SCAs) derived for the period 2010-2021, and compared with H60 elevations. Results indicated that H60 elevations were higher than $Elev_{median\ SCA}$ in most of the study basins and higher than $Elev_{max\ SCA}$ in all basins, regardless of physiographic region. The H60 was not a conservative estimate of the SSZ in most of the Columbia River basin, tending to underpredict the area of the watershed that contributed snow meltwater to peak flow. In watersheds that are more hydrologically sensitive to changes in forest cover, a more conservative estimate of the SSZ may be made using $Elev_{maxSCA}$.

To estimate the SSZ in ungauged basins, random forest regression and correlation analyses were used to identify the most important physical and climatic variables for predicting SSZ elevations. The identified variables were then used to generate linear regression models. In the eastern mountainous physiographic region, the important variables were primarily physical (minimum elevation, longitude and fractional area in two lower to mid-elevation forested biogeoclimatic ecosystem classification (BEC) zones) though one was climatic (number of winter frost-free days). Only climatic variables were identified as important predictors in the western plateau physiographic region, but more data are needed to evaluate the accuracy of the relationships. The residual standard errors for the linear regressions ranged from 71 to 78 m in the western plateau and 171 to 174 in the eastern mountainous regions.

In the eastern mountainous physiographic region, the linear regressions took the form:

$$Elev_{medianSCA\_East} = 8491.11 - 0.029Elev\_Min + 58.46Longitude - 79.19NFFD\_wt \quad (R^2=66\%)$$

$$Elev_{maxSCA\_East} = 812.35 - 495.34MS + 82.44ICH + 0.493Elev\_Min \quad (R^2=65\%)$$

where Elev_Min is the watershed minimum elevation (m); Longitude is the watershed centroid longitude (decimal degrees); NFFD_wt is the average number of winter frost-free days; MS is the

watershed fractional area in the Montane Spruce BEC zone; and ICH is the watershed fractional area in the Interior Cedar Hemlock biogeoclimatic ecosystem zone.

In the western plateau physiographic region, the linear regressions took the form:

$$Elev_{medianSCA\_West} = 2216.18 - 24.36NFFD\_at \text{ } (R^2=65\%)$$

$$Elev_{maxSCA\_West} = 1555.47 - 17.58NFFD\_sp \text{ } (R^2=74\%)$$

where NFFD_at is the mean number of autumn frost-free days; and NFFD_sp is the mean number of spring frost-free days. Because of the small number of stations in the western plateau region, further work is needed to improve these relationships, potentially through the use of naturalised or modelled streamflow records and/or inclusion of stations outside of the Columbia River basin but in the same plateau terrain.

Regression equations for estimating the SSZ in ungauged basins of the upper Columbia River basin in Canada represent an incremental step in reducing the potential impact of industrial activities on watershed processes. Forest management planning that considers snowmelt synchronization across elevation bands in mountainous landscapes can reduce the potential impact on peak flow. The application of SSZ estimates, however, is limited to non-rain on snow (ROS) conditions; further research is needed to better understand the role of forested landscape management on ROS-driven peak flows. Such events may become more common in a warming climate.

The SSZ estimates can also be used to refine cumulative effects analysis of watershed processes. It is important to note that the SSZ represents a long-term average condition, and that the actual snowline in a given year is highly dependent on winter and spring weather. As such, SSZ elevation estimates provide important guidance for strategic level planning, but are not meant to be a rigid threshold above which hydrologic conditions or processes abruptly change. Further work using different data sources and methods, such as other remote sensing products and spatially distributed hydrologic models, are needed to verify the SSZs determined in this study, as well as to predict SSZ extent in ungauged basins outside of the upper Columbia River in Canada.

CONTENTS

FIGURES

TABLES

ACRONYMS

BEC	Biogeoclimatic ecosystem classification
DEM	Digital Elevation Model
$Elev_{max\ SCA}$	Estimated lower limit elevation of the SSZ using maximum snow covered area
$Elev_{median\ SCA}$	Estimated lower limit elevation of the SSZ using median snow covered area
ESSF	Engelmann Spruce-Subalpine Fir BEC
H60	The elevation above which 60% of the watershed area occurs
ICH	Interior Cedar-Hemlock BEC
IDF	Interior Douglas Fir BEC
IMA	Interior Mountain-heather Alpine BEC
IWAP	Interior Watershed Assessment Procedure
LTMAD	Long term mean annual discharge (m^3/s)
MS	Montane Spruce BEC
NFFD	Number of frost-free days
ROS	Rain on snow
SCA	Snow covered area
SNODAS	Snow Data Assimilation System
SSZ	Snow sensitive zone
SWE	Snow water equivalent
USGS	U.S. Geological Survey
WSC	Water Survey of Canada

1. INTRODUCTION

Snow accumulation and melt rates in disturbed forests at mid– and high–elevations of mountainous watersheds may be greater than in adjacent forest stands, increasing the potential for snowmelt synchronization across elevation bands. This may lead to higher peak streamflow, resulting in flooding and damage to communities, infrastructure and ecosystems. Compared to mature forest stands, openings have been found to have 5-70% greater snow water equivalent (SWE) and up to 2 times faster melt rates depending on physical, topographic and meteorological factors, including snowfall magnitude and interannual variations, elevation, aspect, slope, wind speed, specific meteorologic conditions during the melt period, opening size, forest canopy geometry and tree distribution (Jost et al. 2007; Varhola et al. 2010; Boon 2012; Winkler et al. 2015). Change to the forest canopy (usually expressed as amount of area disturbed per watershed) plays an important role in snow accumulation and melt processes. Forest cover change explained 57 and 72% of the variance in the differences in snow accumulation and melt, respectively, across North America and Europe (Varhola et al. 2010). Consideration of snow accumulation and melt processes can be an important component of forestry planning in mountainous catchments, to avoid potential impacts on peak flows.

The snow sensitive zone (SSZ) of a watershed is defined as the area contributing snow meltwater during the peak flow period (Smith et al. 2008). In British Columbia (B.C.), the Interior Watershed Assessment Procedure (IWAP) guidebook (B.C. Ministry of Forests 2001) was developed to help inform forest management planning in snow dominated watersheds. The IWAP provided indicators to assess the distribution of forestry operations by elevation and suggested the use of the H60 (the elevation above which 60% of the watershed area occurs) to identify the area of a watershed from which the majority of the water delivered as peak flow originated. These areas were flagged as having elevated hazards and increased ability to potentially influence a watershed's hydrologic regime in comparison to the lower portions of the watersheds. Harvested areas above the H60 elevation were thus flagged for further exploration by qualified professionals to assess the potential for snowmelt synchronisation within the watershed and associated increases in peak flows. There have been attempts to validate the H60 method in southern B.C., notably Gluns (2001) and Smith et al. (2008). These studies used aerial photography collected sporadically through the melt period, and as a result were expensive, time consuming and were often temporally and spatially limited (although the methods used by Smith et al. (2008) were applied at a regional scale; see Dobson Engineering Ltd. 2003a-c, 2004a-c, 2005a-d and Dobson 2013).

The availability of multi-year, spatial snow cover products has provided the opportunity to assess the SSZ at a broader scale than was possible in the past and to evaluate the H60 approach. Recently, a method was developed and applied in the Kettle River basin in south-central B.C. (Neumann 2022). That analysis used daily gridded SWE products available at 1 km^2 resolution for southern B.C. through the National Snow and Ice Data Centre (Barrett 2003; NOHRSC 2004). The Snow Data Assimilation System (SNODAS) integrates information from weather forecast and snow process models with remote sensing and ground observations to simulate snow cover across the contiguous United States and parts of southern Canada. SNODAS products were developed and have been used as inputs (or to derive inputs) to hydrologic models for river forecasting and water resource planning (Bair et al. 2013; Guan et al. 2013a; Pomeroy et al. 2015; Driscoll et al. 2017; Hammond et al. 2018; Massmann 2019; Arsenault et al. 2020), but have been widely used as validation datasets for weather models, remotely sensed data and field measurements (Lea 2007; Tedesco and Narvekar 2010; Clow et al. 2012; Artan et al. 2013; Guan et al. 2013b; Schneiderman et al. 2013; Vuyovich et al. 2014; Boniface et al. 2015; Hedrick et al. 2015; Zheng et al. 2015; Bair et al. 2016; Broxton et al. 2016; X. Liu et al. 2016; Wrzesien et al. 2017; Keum et al. 2018; Musselman et al. 2018; Siren et al. 2018; X. Liu et al. 2019; Zahmatkesh et al. 2019; Gan et al.

2021). The high temporal resolution of the SNODAS products make it especially useful during the snowmelt period when conditions can change rapidly, and the 1 km^2 resolution is appropriate for studies of medium sized to large watersheds (>50 km^2). The relatively wide use in the literature and availability of data back to 2010 were also considerations in selecting the SNODAS dataset for this analysis.

Neumann (2022) found that using a fixed snow covered area (e.g., the H60) without consideration of basin characteristics did not adequately estimate the SSZ. That conclusion led to the current study of snowline elevations across the upper Columbia River basin in Canada to explore relationships with topographic and climatic drivers that control snow accumulation and melt. The objectives of this analysis were to estimate the lower limit elevation of the SSZ for gauged basins in the upper Columbia River watershed, and to identify physical and climatic factors that could be used to estimate the snowline elevation in ungauged basins. Attention was focussed on factors that could be easily derived operationally using simple GIS analysis or publicly available online tools. Being able to estimate the SSZ for watersheds across the upper Columbia River basin is an incremental advance in the consideration of potential forest harvest and disturbance impacts on spring peak flows, such as for watershed and landscape level resource management plans.

2. MATERIALS AND METHODS

The upper Columbia River basin in Canada (approx. 102,000 km^2) is a mountainous landscape with numerous large valley reservoirs used for hydroelectric power generation. The complex topography combined with prevailing wind direction and orographic forcing effects result in a wide range of climates and ecosystems, including grasslands and dry pine forests, interior rain forests, alpine meadows and glaciers. Forest harvest activities in the basin accelerated after 1900 (Gayton and Wrangler 2003) and forestry continues to be an active economic sector. Forest cover in the basin has also been impacted by wildfires, insect outbreaks and mining, creating a complex pattern and timeline of forest disturbance.

For this study, 57 gauged basins categorized as having a “natural” flow type in the Water Survey of Canada (WSC) HYDAT database were selected in the upper Columbia River basin (Figure 1). While the “natural” category does not infer that flow is not impacted by withdrawals and other human activities, it is assumed that the streamflow pattern is similar to what would occur without regulation. Systems categorised as “regulated” in the HYDAT database have physical flow control structures that alter streamflow in more than 5% of the basin area (Brimley et al. 1999).

The selected basins spanned a wide range of climates, sizes (51.7 – 10,009 km^2) and mean elevations (1290 – 2028 m) (Table 1). The spatial resolution of the SNODAS data (1 km^2) limited the analysis to medium to large watershed areas; in most cases, however, small gauged watersheds were nested within the ones selected and so were represented in the dataset. Some of the watersheds in the northeastern part of the study area included substantial alpine area and glaciers, while many in the southwest were forested to their highest elevations. Total snowfall increased with elevation, and higher precipitation amounts occurred in the northeast and southeast regions of the basin. Regulated systems where there were relatively large reservoirs and dams were excluded from the analysis.

The stations were divided into two physiographic regions (Figure 1 and Table 1); stations in the western part of the study area fell within the Shuswap and Okanagan Highlands and the Thompson Plateau physiographic regions (n = 15), while those in the eastern part were in the Columbia Mountains and Rocky Mountains physiographic regions (n = 42) (Moore and McKendry 1996; Church and Ryder 2010). Physiography can be a significant control on snowmelt rates and patterns; elevation, slope and aspect

would have less influence on orographic precipitation and snowmelt in areas of flatter topography in the headwaters of basins in the western plateau region and therefore on the extent and location of the SSZ. This was expected to contrast with the strong influence of slope and aspect in the eastern mountainous region. The boundary between the two regions was adopted from the physiographic areas layer in the BC Data Catalogue (https://catalogue.data.gov.bc.ca/dataset/physiographic-areas).

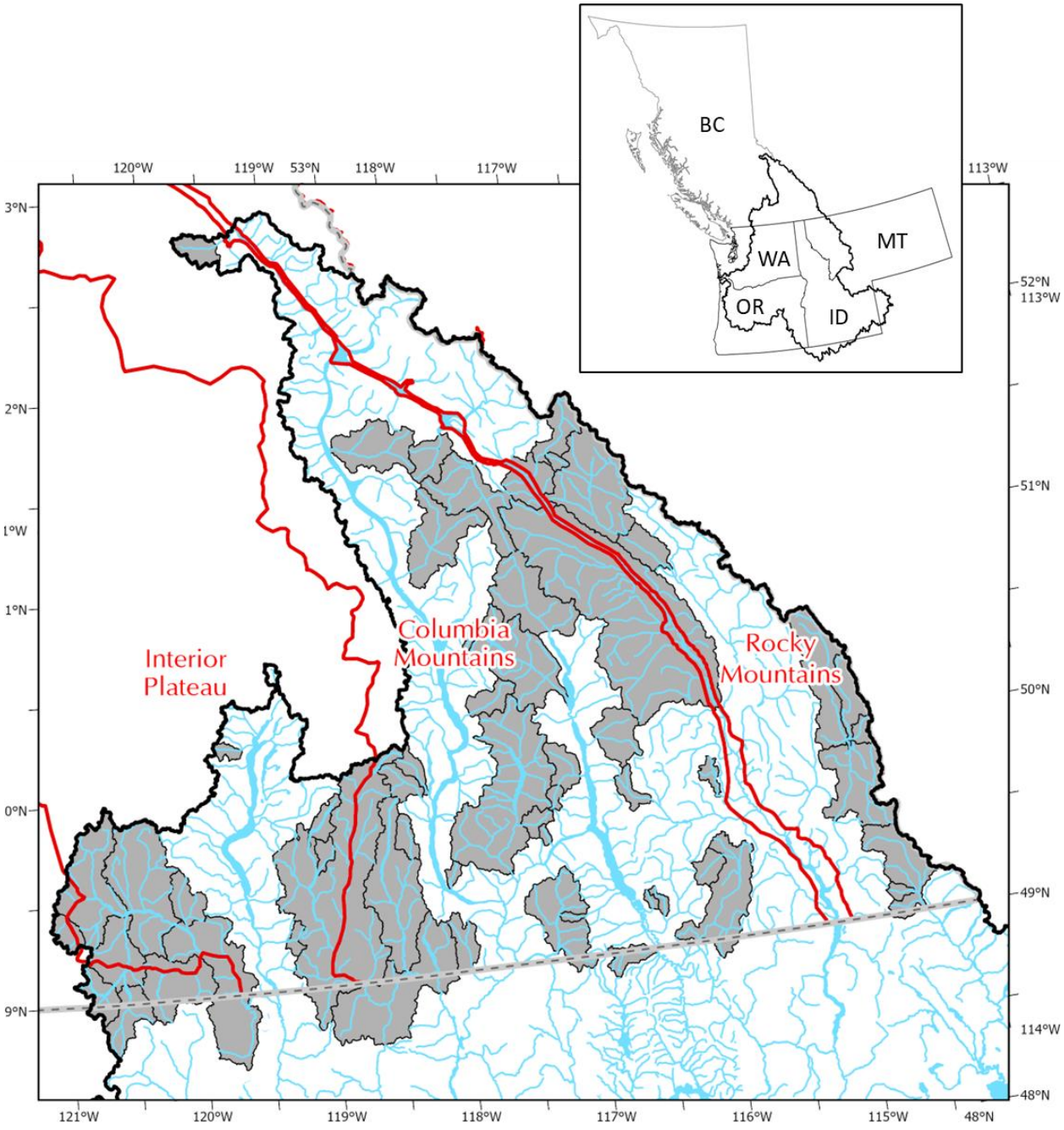

Figure 1. Map of study basins (grey) in the upper Columbia River basin in British Columbia. Major water features are shown in blue, and approximate boundaries between primary physiographic regions in red. The inset map shows the extent of the Columbia River basin in western North America.

Table 1. Name and geographic information for the 57 study basins in the upper Columbia River basin. Shading indicates watersheds in the western plateau region, while the remaining basins were in the eastern mountainous region.

Basin	WSC Station ID	Area (km^2)	Longitude (decimal degrees)	Latitude (decimal degrees)
Arrow Creek	08NH084	79.2	-116.462	49.23199
Beaton Creek	08NE008	94.9	-117.682	50.67112
Beaver River	08NB019	1,156.7	-117.529	51.35108
Big Sheep Creek	08NE039	346.8	-117.983	49.14832
Blaeberry River	08NB012	589.5	-116.773	51.61341
Boundary Creek*	08NH032	253.8	-116.758	48.9774
Cabin Creek	08NP004	96.1	-114.655	49.10713
Canoe River	08NC004	310.6	-119.529	52.72118
Columbia River at Donald	08NB005	9,719.0	-116.543	50.92155
Columbia River at Nicholson	08NA002	6,647.5	-116.471	50.69757
Deer Creek	08NE087	82.6	-118.007	49.49453
Duck Creek	08NH016	51.7	-116.533	49.24246
Duhamel Creek	08NJ026	54.8	-117.275	49.63419
Duncan River	08NH119	1,304.7	-117.166	50.81503
Elk River at Fernie	08NK002	3,099.1	-114.895	49.97742
Elk River near Natal	08NK016	1,847.6	-114.928	50.18313
Flathead River *	08NP001	1,103.1	-114.622	49.22554
Fording River	08NK018	620.8	-114.795	50.07661
Fry Creek	08NH130	583.9	-116.622	50.085
Gold River	08NB014	420.7	-117.823	51.56931
Goldstream River	08ND012	938.0	-118.251	51.65253
Hidden Creek	08NE114	56.7	-117.15	49.21152
Illecillewaet River	08ND013	1,149.2	-117.832	51.17105
Kaslo River	08NH005	440.4	-117.092	49.93432
Keen Creek	08NH132	93.2	-117.162	49.81738
Kicking Horse River	08NA006	1,847.3	-116.552	51.3337
Kootenay River at Kootenay Crossing	08NF001	425.9	-116.21	50.99066
Kuskanax Creek	08NE006	318.8	-117.565	50.34211
Lardeau River	08NH007	1,634.5	-117.325	50.52303
Lemon Creek	08NJ160	179.3	-117.326	49.7092
Line Creek	08NK022	137.9	-114.743	49.92924
Mather Creek	08NG076	139.1	-115.952	49.82446
Moyie River above Negro Creek	08NH120	238.3	-116.062	49.36544
Moyie River at Eastport*	08NH006	1,565.0	-115.987	49.22787
Salmo River	08NE074	1,246.7	-117.217	49.21467
Slocan River	08NJ013	3,329.9	-117.529	49.86583
Split Creek	08NB016	79.5	-116.817	51.47595
St. Mary River	08NG077	211.0	-116.58	49.80545
Ashnola River	08NL004	1,053.9	-120.191	49.07966
Barnes Creek	08NE077	198.6	-118.233	50.04425
Burrell Creek	08NN023	221.5	-118.337	49.70113
Granby River	08NN002	2,062.3	-118.448	49.46456
Hedley Creek	08NL050	390.2	-120.062	49.49282
Inonoaklin Creek	08NE110	290.6	-118.337	49.97818

Table 1 Continued. Name and geographic information for the 57 study basins.

Basin	WSC Station ID	Area (km^2)	Longitude (decimal degrees)	Latitude (decimal degrees)
Kettle River near Ferry, WA*	08NN013	5,663.4	-118.897	49.4849
Kettle River near Laurier, WA*	08NN012	10,009.4	-118.719	49.35884
Pasayten Creek	08NL069	564.6	-120.574	48.93178
Similkameen River above Goodfellow Creek	08NL070	426.1	-120.767	49.05195
Similkameen River at Princeton	08NL007	1,809.0	-120.638	49.10345
Similkameen River near Hedley	08NL038	5,569.0	-120.604	49.42859
Similkameen River near Nighthawk, WA*	08NL022	9,115.7	-120.361	49.30743
Trapping Creek	08NN019	148.0	-118.977	49.66372
Tulameen River at Princeton	08NL024	1,777.9	-120.811	49.57678
Tulameen River below Vuich Creek	08NL071	251.9	-120.988	49.37364
Vaseux Creek	08NM171	117.9	-119.255	49.25059
West Kettle River near McCulloch	08NN015	231.4	-118.953	49.82582
Whiteman Creek	08NM174	107.6	-119.655	50.21675

The method used to estimate the SSZ for each study basin is summarised in Figure 2. The approach used a combination of streamflow (hydrometric) data and the publicly available SNODAS SWE product. Details of each component are provided below.

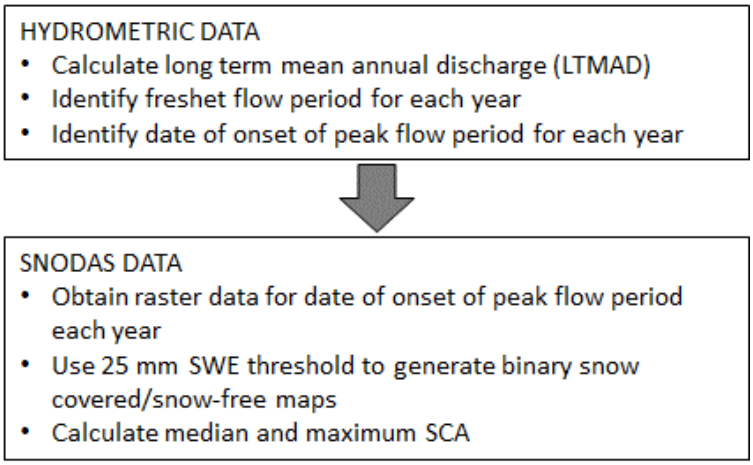

Figure 2. Method used to estimate the snow sensitive zone for gauged watersheds, using hydrometric and SNODAS data.

Hydrometric data for 2010-2020 for the selected stations were acquired from the WSC online database (approved data; https://wateroffice.ec.gc.ca/mainmenu/historical_data_index_e.html last accessed 6 April 2023) and directly from WSC staff (provisional data) (Table 1 and Figure 1). Six stations in the U.S. are cooperatively managed by WSC and USGS, and data for these stations were available from the WSC online database. While most of the systems selected for this analysis have provincially licensed water withdrawals, they were all listed as having a "natural" flow type in the WSC database. Licensed withdrawal volumes would be small relative to the flows occurring during the freshet period, which is the focus of this study.

In many cold continental or high elevation watersheds where snowmelt is the primary driver of peak flow, the hydrograph would be expected to have a single annual peak (Gluns 2001; Tennant et al. 2014). In the temperate climate of southern B.C. and in watersheds that span a wide range of elevations, freshet hydrographs tend to have multiple peaks, sometimes of similar magnitude, influenced by periods of rapid snowmelt, rainfall and/or rain-on-snow events (Gluns 2001; Tennant et al. 2014). When assessing the hydrometric data, then, the date of onset of the peak flow period was used instead of the peak flow date, following the approach used by Smith et al. (2008). For each station, every year of hydrometric data was analysed to identify the start and end dates of the freshet flow period, defined as when the daily mean discharge was greater than the long-term mean annual discharge (LTMAD) for that station. Most of the stations had records between 1985 and 2014 (30 years), so this period was used to calculate the LTMAD. Gaps in incomplete datasets were ignored and the mean was calculated using all available values between 1985 and 2014 (for stations with data gaps, the number of missing years is indicated under LTMAD in Table 3). The date when discharge exceeded the LTMAD for five or more consecutive days was identified as the start of the freshet flow period, and the last date that flow remained above the LTMAD was the end of the freshet flow period (Smith et al. 2008). The start date of each peak flow period was then identified as the date when the daily mean discharge was greater than the mean for that freshet flow period (Smith et al. 2008) (Figure 3 and Figure 4).

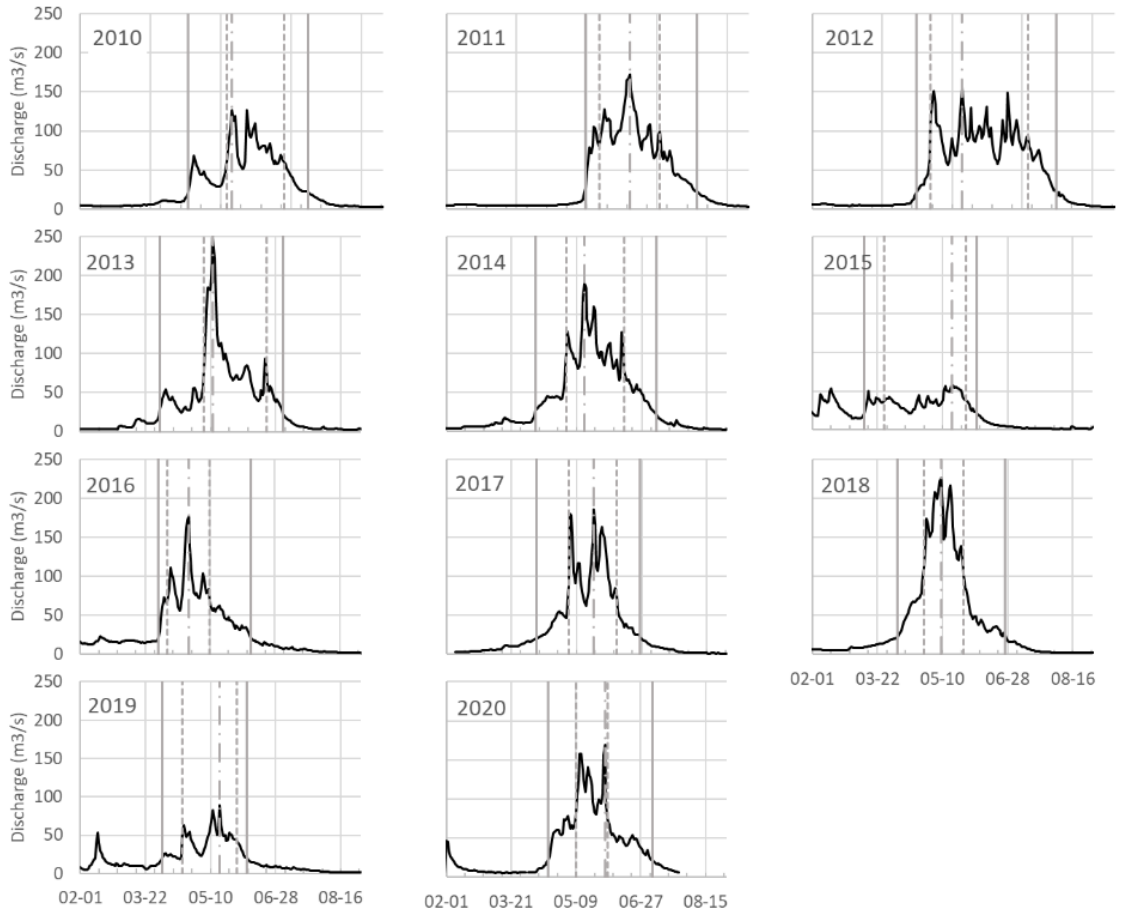

Figure 3. Example freshet period hydrographs for Tulameen River at Princeton (WSC ID 08NL024) in the western plateau physiographic region. The start and end dates for the freshet (solid line) and peak flow (dashed line) periods are shown with the date of peak flow (dot-dashed line).

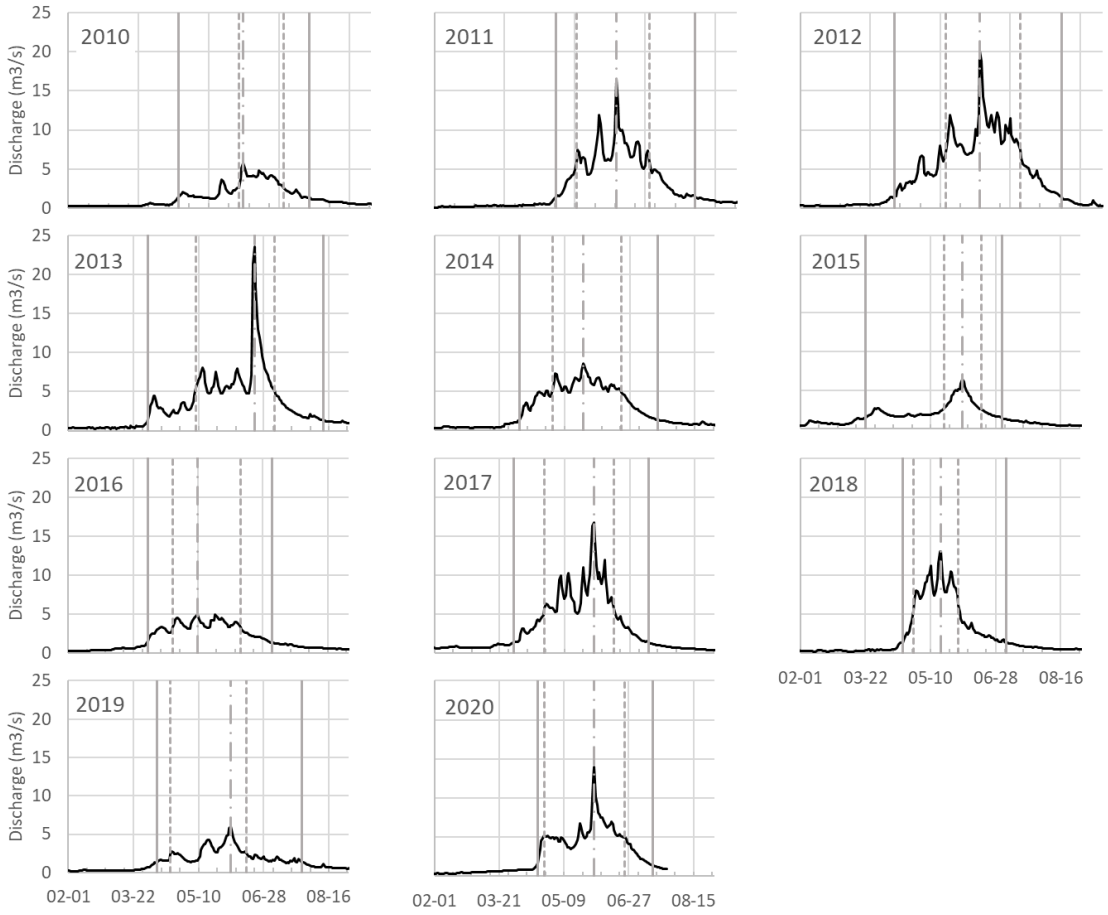

Figure 4. Example freshet period hydrographs for Mather Creek below Houle Creek (WSC ID 08NG076) in the eastern mountainous region. The start and end dates for the freshet (solid line) and peak flow (dashed line) periods are shown with the date of peak flow (dot-dashed line).

Watershed snow covered areas (SCA) for each of the 2010-2020 peak flow start dates were derived from SNODAS daily SWE data products (Barrett 2003; NOHRSC 2004). Unmasked tar files were retrieved from the National Snow and Ice Data Center (ftp://sidads.colorado.edu/DATASETS/NOAA/G02158/). The daily products represent conditions at 06:00 UTC, which is 22:00 Pacific Standard Time, so the date stamp in the file name had to be matched carefully with the date needed for analysis. A Python script was written to uncompress the tar files and extract the SWE product (Product Code 1034), which then had to be uncompressed. Header files were created for each SWE product file following Barrett (2003) and online instructions (https://nsidc.org/support/how/how-do-i-import-snodas-data-arcgis last accessed on 25 May 2021). The SWE data was imported to ArcGIS, reprojected and subset to cover the study area. Binary maps of snow-covered and snow-free pixels were derived using a 25 mm SWE threshold (pixels with less than 25 mm SWE were considered snow-free) (Neumann 2022). The binary maps were clipped to the watershed boundaries and SCA was calculated as the area of all snow covered pixels and sub-pixels divided by the watershed area, expressed as a percent. In previous analysis, the median SCA was used to estimate the SSZ area in order to reduce the influence of extreme values. A potentially more conservative approach to estimating the SSZ area, which may be an appropriate choice in hydrologically sensitive watersheds, is to use the maximum SCA. Both statistics were calculated in this study, and results compared.

Physical and climatic variables were derived for each watershed following Pike and Wilford (2013) (Table 2). Physical characteristics were calculated using GIS software and included:

- watershed area (km^2, using the B.C. Freshwater Atlas watersheds, https://catalogue.data.gov.bc.ca/dataset/freshwater-atlas-watersheds last accessed 6 April 2023);
- latitude and longitude of the watershed centroid (decimal degrees);
- the percent watershed area in four major forested biogeoclimatic ecosystem classification (BEC) zones (Engelmann Spruce-Subalpine Fir (ESSF), Interior Cedar-Hemlock (ICH), Interior Douglas Fir (IDF) and Montane Spruce (MS)) and the Interior Mountain-heather Alpine (IMA) BEC zone (version 12, https://catalogue.data.gov.bc.ca/dataset/bec-map last accessed 6 April 2023);
- maximum, minimum and mean watershed elevation derived from a 25 m Digital Elevation Model (DEM) for B.C. (https://catalogue.data.gov.bc.ca/dataset/digital-elevation-model-for-british-columbia-cded-1-250-000 last accessed 6 April 2023); for the U.S., the 10 m USGS DEM was resampled to 25 m resolution before being combined with the B.C. DEM (https://apps.nationalmap.gov/downloader/#/ last accessed 6 April 2023);
- mean slope derived from the DEM;
- the percent watershed area with north, east, south, west and flat aspects, derived from the DEM, and;
- the percent watershed area that was forested, covered by snow/ice or unvegetated (retrieved from watershed reports in the BC Kootenay Boundary Water Tool, https://kwt.bcwatertool.ca/watershed last accessed 18 April 2023).

Table 2. Watershed physical and climatic properties used as independent variables in the random forest regression.

Category	Variable	Details
Physical	Watershed area (km^2)	Derived from B.C. Freshwater Atlas
	Longitude, Latitude (decimal degrees)	Derived for watershed centroid
	Biogeoclimatic ecosystem classification (BEC) zone	% of watershed area in major BEC zones ESSF, ICH, IDF, IMA and MS*
	Maximum, minimum, mean and range in watershed elevation (m)	Derived from 25 m DEM
	Slope	Mean for watershed
	Aspect – North, East, South, West, Flat	% of watershed area in each quadrant, derived from 25 m DEM
	Forest, snow/ice and unvegetated land cover	% of watershed area with each landcover type
Climatic	Total precipitation (mm)	Annual and seasonal
	Mean air temperature (°C)	Annual, seasonal and monthly (April, May and June)
	Precipitation as snow (mm)	Annual and seasonal
	Number of frost-free days (NFFD)	Annual and seasonal
	Degree days less than zero	Annual and seasonal
	Continentality	Warmest month minus coldest month

*ESSF = Engelmann Spruce-Subalpine Fir; ICH = Interior Cedar Hemlock; IDF = Interior Douglas Fir; IMA = Interior Mountain-heather Alpine; MS = Montane Spruce.

Climatic characteristics were derived with the desktop ClimateNA application (v. 7.01; Wang et al. 2016; https://climatena.ca/ last accessed 6 April 2023) using the most recent 1991-2020 normal period, which overlaps with the period used to calculate LTMAD for each station (1985-2014). The centroid latitude and longitude and the watershed mean elevation were used as inputs. Climatic variables included in this analysis were:

- annual and seasonal total precipitation (mm);
- annual, seasonal and spring monthly (April, May and June) air temperature (°C);
- annual and seasonal precipitation as snow (mm);
- annual and seasonal average number of frost-free days (NFFD);
- annual and seasonal degree days below 0°C; and
- a continentality index (calculated as the difference between the mean temperature of the hottest month and the mean temperature of the coldest month).

Hypsometric curves for each basin were based on the DEMs using the Hypsometric Integral Toolbox for ArcGIS (Matos and Dilts 2019).

Forty-eight physical and climatic variables were used in random forest regressions to assess their importance in explaining the SSZ elevation (R *randomForest()* function in the *randomForest* package v. 4.7-1.1, using 500 trees; Liaw and Wiener 2002). Random forest models are useful in analyses with multiple, non-linear relationships, and are commonly used to assess the influence of each independent variable. The most important variables were identified using two importance measures – the mean increase in node purity, and the percent increase in mean square error. The most important variables were then used in a multiple linear regressions to estimate the SSZ elevation (R *lm()* function in the *stats* package v. 4.2.2; R Core Team 2022).

Where a sample size was too small for random forest regression analysis, a single predictor variable was identified using correlation analysis. The physical or climatic variable with the strongest correlation coefficient (positive or negative) was used in subsequent linear regression analysis. The analysis was limited to a single factor because of the small sample size, the high risk of overfitting, and there being no justification for a more complex equation.

As a result, four linear regressions were developed to predict the SSZ determined using the median SCA ($Elev_{medianSCA}$) and using the maximum SCA ($Elev_{maxSCA}$) in the eastern mountainous and western plateau regions of the study area. Graphs were produced using the *plot()* and *dotchart()* functions in the default R *graphics* package (version 4.2.2) as well as the ggplot2 package (version 3.4.2, Wickham 2016) .

3. RESULTS

3.1 Hydrometric Data Analysis

The hydrographs for the selected watershed showed multiple peaks in most years, often of similar magnitude (example hydrographs for the Tulameen River at Princeton (WSC ID 08NL024) and Mather Creek below Houle Creek (08NG076) are shown in Figure 3 and Figure 4). Annual peak flow period start dates were derived for 57 hydrometric stations in the upper Columbia River basin in Canada (Table 3 and Figure 5). Snowmelt-driven peak flows began later in the north-eastern portion of the study region and in higher elevation headwater basins.

Table 3. Hydrometric results and SSZ elevations for the 57 study basins in the upper Columbia River basin. LTMAD is the station long term (30 year) mean annual discharge. Shading indicates watersheds in the western plateau region, while the remaining basins were in the eastern mountainous region.

Basin	LTMAD (m^3/s) (# missing years)	Mean Peak Flow Period Onset (DOY)	Median SSZ Elev. (m)	Min. SSZ Elev. (at max SCA) (m)	H60 Elev. (m)
Arrow Creek	1.7	6 May (126)	1345	940	1485
Beaton Creek	2.6 (3)	10 May (130)	1000	<444	1330
Beaver River	42.0	21 May (141)	1115	830	1751
Big Sheep Creek	5.2	21 April (111)	990	925	1400
Blaeberry River	16.7 (3)	21 May (141)	1535	<845	1860
Boundary Creek*	5.7 (3)	5 May (125)	1155	825	1420
Cabin Creek	2.0	10 May (130)	1400	<1294	1730
Canoe River	14.9 (3)	5 June (156)	1605	990	1795
Columbia River at Donald	166.6	27 May (147)	1775	1460	1620
Columbia River at Nicholson	105.9	30 May (150)	1805	1490	1560
Deer Creek	0.9	6 May (126)	1010	640	1210
Duhamel Creek	1.5 (11)	8 May (128)	845	<713	1450
Duck Creek	0.9	11 May (131)	1350	1120	1445
Duncan River	62.0	16 May (136)	1020	740	1795
Elk River at Fernie	47.3	15 May (135)	1690	1355	1765
Elk River near Natal	25.5	21 May (141)	1745	1315	1865
Flathead River *	24.3 (10)	11 May (131)	1463	1280	1694
Fording River	8.1	17 May (137)	1700	1475	1885
Fry Creek	19.3	17 May (137)	1025	<833	1930
Gold River	18.1	28 May (148)	1250	945	1965
Goldstream River	38.0	18 May (138)	850	645	1555
Hidden Creek	1.6	4 May (124)	965	<693	1475
Illecillewaet River	52.4	16 May (136)	1115	<507	1625
Kaslo River	12.8	17 May (137)	1055	780	1670
Keen Creek	3.3	17 May (137)	<1205	<1205	1895
Kicking Horse River	40.4	23 May (143)	1730	1170	1785
Kootenay River at Kootenay Crossing	4.8	19 May (139)	1550	<1158	1465
Kuskanax Creek	13.4	16 May (136)	815	<606	1585
Lardeau River	56.9 (7)	18 May (138)	1020	635	1570
Lemon Creek	4.6	14 May (134)	1000	<541	1620
Line Creek	2.1	16 May (136)	1830	1535	1895
Mather Creek	1.3	1 May (121)	1395	1215	1385
Moyie River above Negro Creek	4.5	6 May (126)	1290	<1083	1630
Moyie River at Eastport*	18.4	28 April (118)	1245	990	1384
Salmo River	31.3	4 May (124)	1110	780	1380
Slocan River	91.0	17 May (137)	1160	875	1470
Split Creek	1.7 (2)	22 May (142)	1630	<973	1885
St. Mary River	7.2	17 May (137)	<1061	<1061	1780
Ashnola River	7.3	11 May (131)	1380	1270	1810
Barnes Creek	3.8	9 May (129)	1235	800	1435

Table 3 Continued. Hydrometric results and SSZ elevations for the 57 study basins.

Basin	LTMAD (m^3/s) (# missing years)	Mean Peak Flow Period Onset (DOY)	Median SSZ Elev. (m)	Min. SSZ Elev. (at max SCA) (m)	H60 Elev. (m)
Burrell Creek	4.2	1 May (121)	<901	<901	1380
Granby River	29.7	3 May (123)	1130	835	1230
Hedley Creek	2.4	4 May (124)	1265	1195	1635
Inonoaklin Creek	3.7 (3)	6 May (126)	1065	605	1395
Kettle River near Ferry, WA*	44.1	1 May (121)	1220**	1045	1250
Kettle River near Laurier, WA*	82.5	2 May (122)	1270	1085	1195
Pasayten Creek	8.0 (1)	10 May (130)	<1044	<1044	1635
Similkameen River above Goodfellow Creek	7.7 (2)	11 May (131)	<1071	<1071	1600
Similkameen River at Princeton	22.5	6 May (126)	1140	800	1495
Similkameen River near Hedley	48.1	1 May (121)	1110	855	1345
Similkameen River near Nighthawk, WA*	63.0 (1)	3 May (123)	1250	1040	1385
Trapping Creek	1.4	27 April (117)	1120	<880	1295
Tulameen River at Princeton	20.7	2 May (122)	1010	770	1275
Tulameen River below Vuich Creek	6.6	10 May (130)	<1028	<1028	1505
Vaseux Creek	0.9	4 May (124)	1360	<1179	1650
West Kettle River near McCulloch	3.4	10 May (130)	1170**	<1024	1580
Whiteman Creek	0.6 (2)	20 April (110)	1070	865	1390

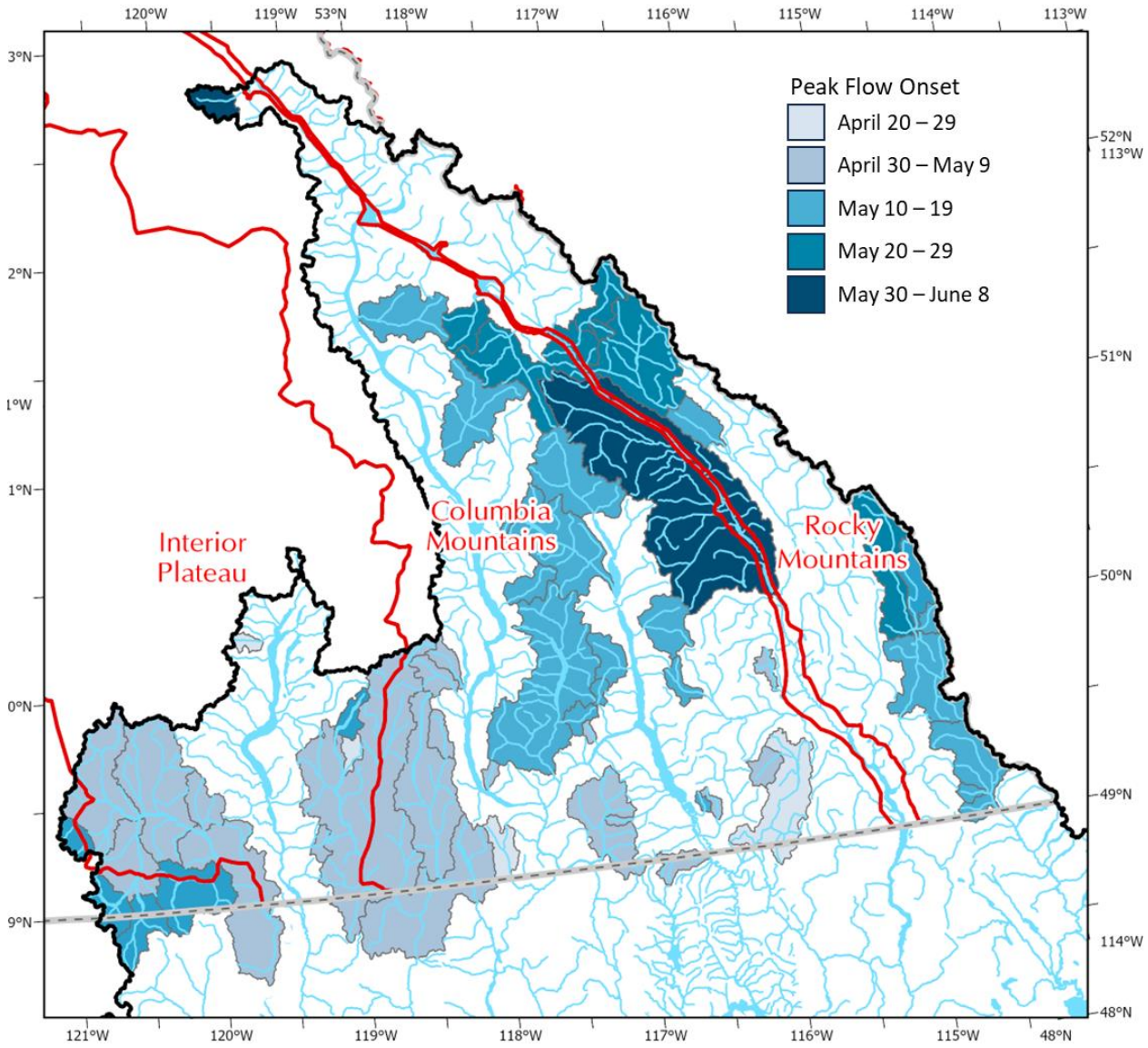

Figure 5. Peak flow onset dates across the study area. The approximate boundaries between physiographic regions are shown in red.

3.2 Snow Sensitive Zone Delineation

The snow-covered fractions at the start of each peak flow period were calculated. Example maps for watersheds in the western plateau (Tulameen River watershed) and the eastern mountainous regions (Mather Creek watershed) are shown in Figure 6 and Figure 7. In both regions, SCA values varied considerably from year to year depending on winter snow accumulation and winter and spring melt events. The 2015 season was particularly distinctive, especially in the western and southern portions of the study region. A "warm blob" of ocean water persisted off the coast of B.C. through the winter and spring. January, February and March were much warmer than normal, and more precipitation fell as rain at lower elevations. As a result, the snowpack was gone from low and mid-elevations by April (B.C. River Forecast Centre 2015). The remaining snow at higher elevations melted rapidly due to very warm temperatures in May and rain from convective storms. The effect in this analysis was the identification of either a very early date for the peak flow period onset (e.g., 7 February 2015 for the Salmo River at

Salmo compared to the median date of 4 May, WSC ID 08NE074) or a very low SCA (e.g., SCA in the West Kettle River basin above Westbridge was 9% in 2015 compared to the median value of 74%, WSC ID 08NN003). The effect was diminished in the north-eastern parts of the study region. Using the median SCA (rather than the mean) to estimate the lower elevation of the SSZ reduced the influence of this anomalous year on the SSZ estimates.

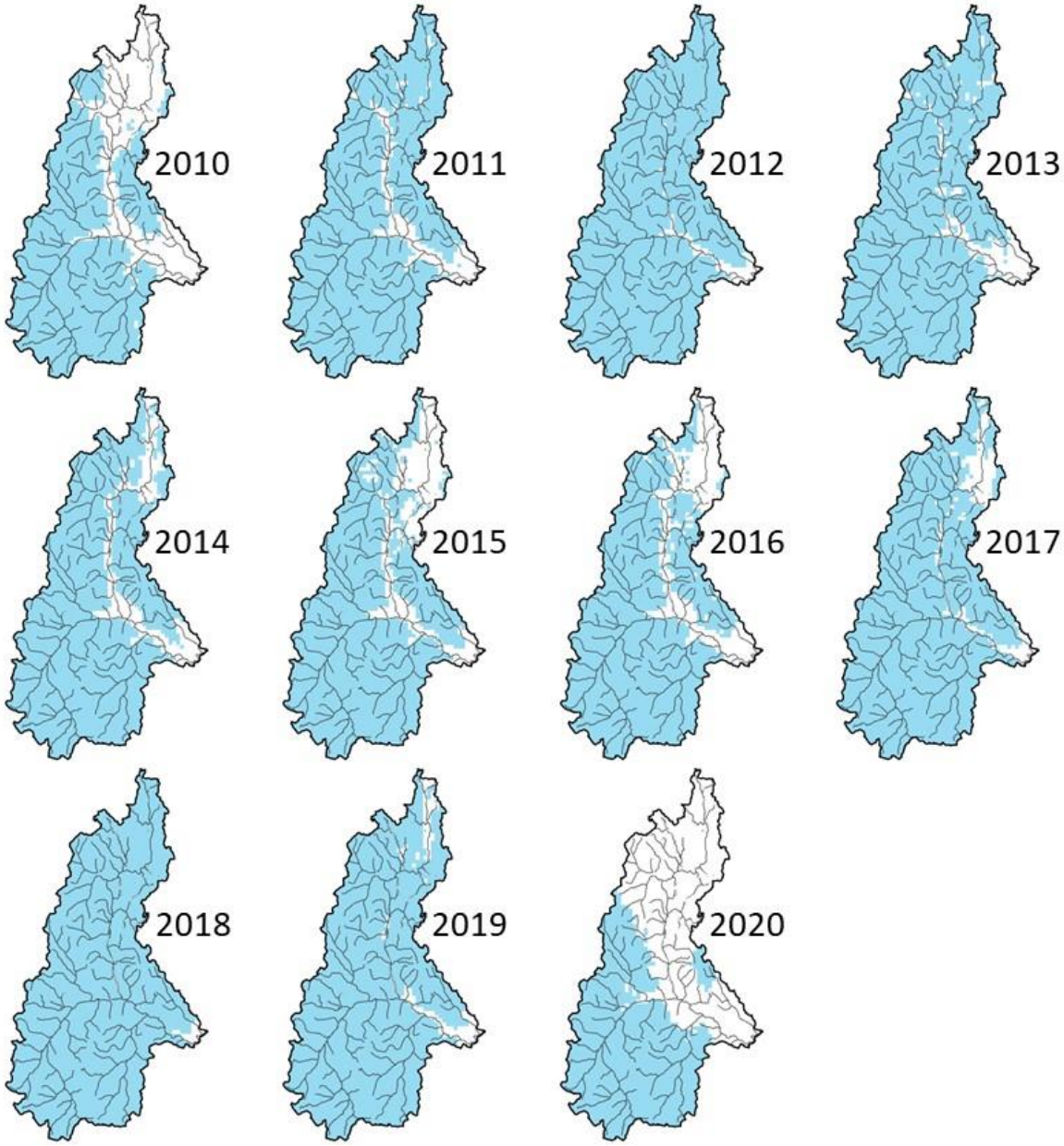

Figure 6. Variation in snow covered area (blue) at the start of the peak flow period for the Tulameen River watershed at Princeton (WSC ID 08NL024) in the western plateau physiographic region. SCA was closest to the median value of 91% in 2011. Stream channels are shown.

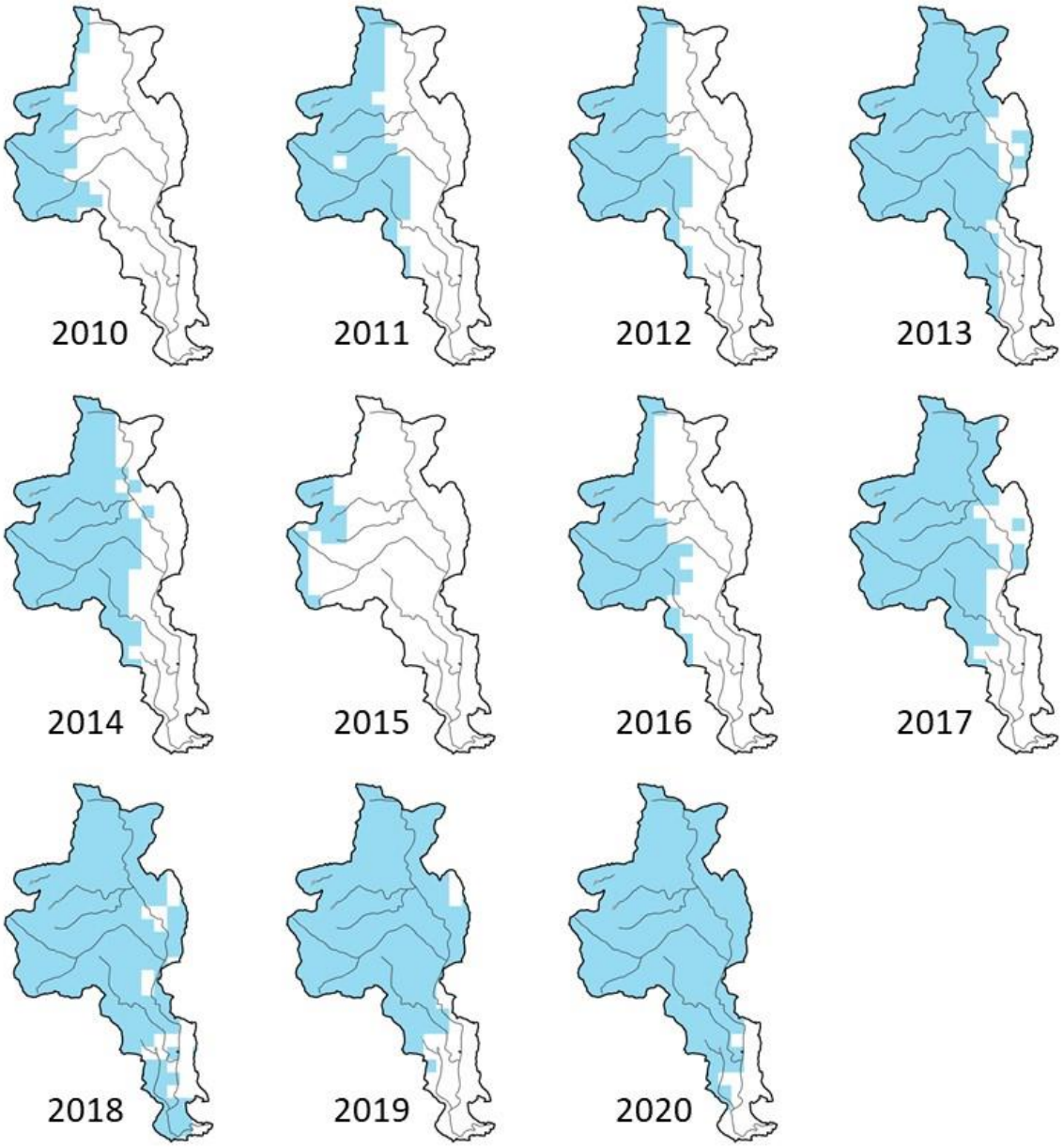

Figure 7. Variation in snow covered area (blue) at the start of the peak flow period for the Mather Creek watershed below Houle Creek (WSC ID 08NG076) in the eastern mountainous physiographic region. SCA was closest to the median value of 58% in 2014. Stream channels are shown.

The median and maximum SCA for the 2010-2020 period were calculated for each basin and used with its hypsometric curve to estimate the corresponding elevations of the lower limit of the SSZ ($Elev_{medianSCA}$ and $Elev_{maxSCA}$ in Table 2 and Figure 8). The median and maximum SCA values in 9 and 29 of the study basins, respectively, were 99-100% of the total basin area, indicating that the lower limit of the SSZ was at or below the minimum basin elevations. Results for these stations were removed from the regression analysis. In the remaining watersheds, the mean difference between $Elev_{medianSCA}$ and $Elev_{maxSCA}$ was 281 m, ranging between 65 and 615 m.

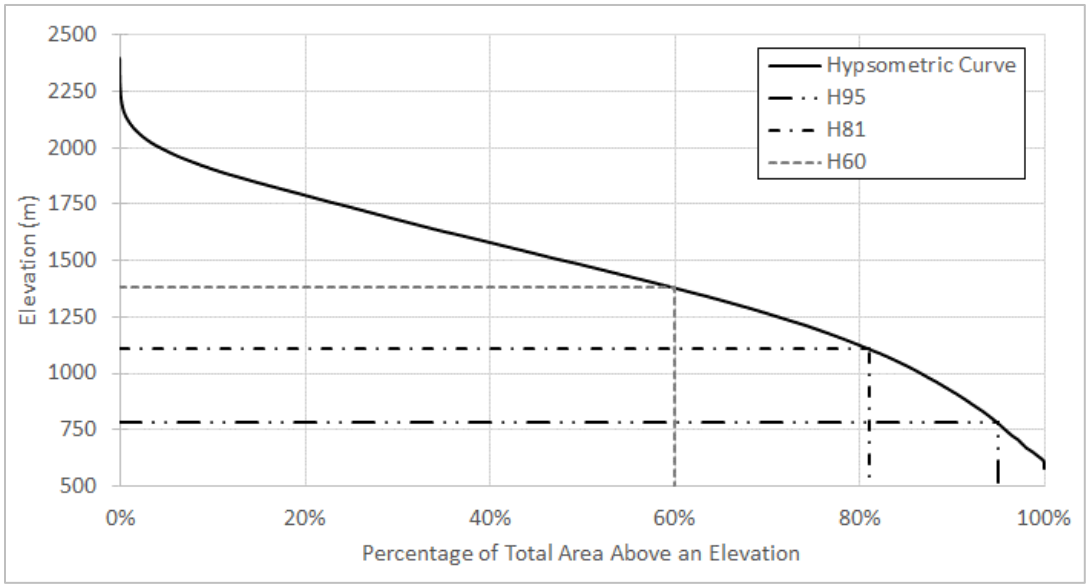

Figure 8. Hypsometric curve for the Salmo River watershed above Salmo (WSC ID 08NE074) showing the lower elevation of the snow sensitive zone calculated using the maximum SCA (H95) and the median SCA (H81), and the H60 elevation.

The H60 elevations were also estimated from the hypsometric curves for comparison (Table 2). In the majority of the study basins, the H60 elevation was higher than that found for the SSZ lower limit using the median SCA (Figure 9, left). The comparison between the H60 elevations and those determined using the maximum SCA was limited to 28 watersheds where the SCA was less than 99% at the start of the peak flow period, predominantly at lower elevations (Figure 9, right). However, the H60 elevations were never lower than those determined using the maximum SCA.

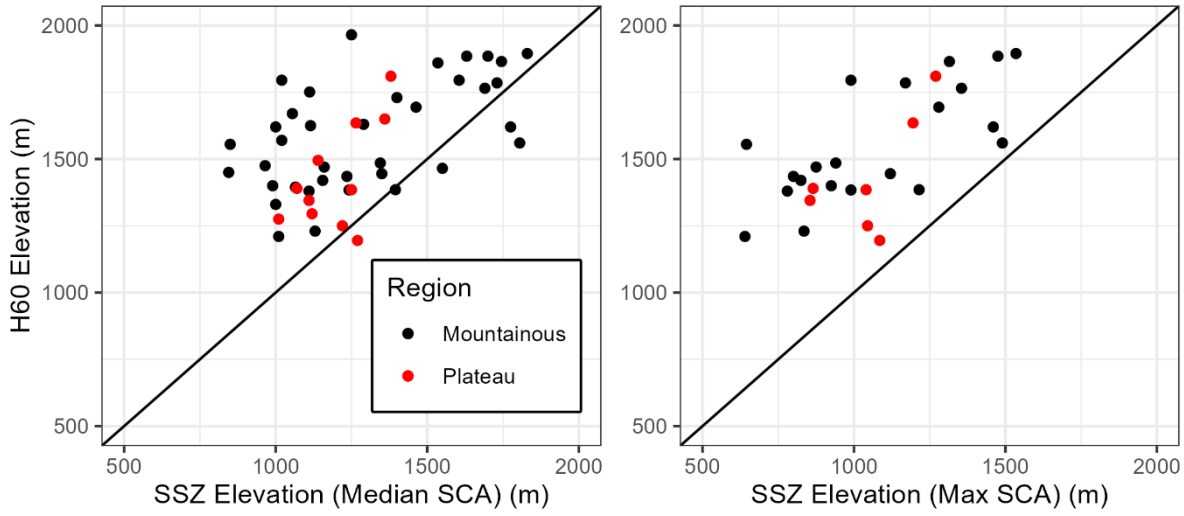

Figure 9. Comparison of H60 and SSZ lower limit elevations calculated using (left) median SCA and (right) maximum SCA at the start of the peak flow period. The 1:1 line is shown in each graph.

3.3 Regression Analysis

3.3.1 Eastern Mountainous Region

SSZ from the Median SCA

Random forest regression was used to identify the most important physical and climatic variables for predicting SSZ elevation in the eastern mountainous region using the median SCA (n = 37, residual standard error = 170 m, variance explained = 66%). Three factors were identified whose exclusion increased the mean square error by >8%: minimum elevation (Elev_Min), longitude (Longitude) and the number of frost-free days in the winter (NFFD_wt) (Figure 10 and Figure 11). The same factors topped the list of variables that increased node purity, though in a different order and with longitude listed as fourth most important. The linear regression model using Elev_Min, Longitude and NFFD_wt had an adjusted R^2 value of 66% and residual standard error of 174 m ($p<0.01$), similar to the random forest regression results, and had the form:

$$Elev_{median\ SCA\_East} = 8491.11 - 0.0427Elev\_Min + 66.04Longitude - 80.02NFFD\_wt$$

where $Elev_{medianSCA\_East}$ is the lower limit elevation of the SSZ estimated using the median SCA value for the eastern physiographic region. Adding the fractional area of each watershed within the Interior Cedar – Hemlock BEC zone (ICH), as was indicated when variable importance was assessed using the 'increase in node purity' metric (Figure 10, right), did not improve the amount of variability explained (adjusted R^2 = 64%) nor the residual standard error (180 m), so this variable was not included.

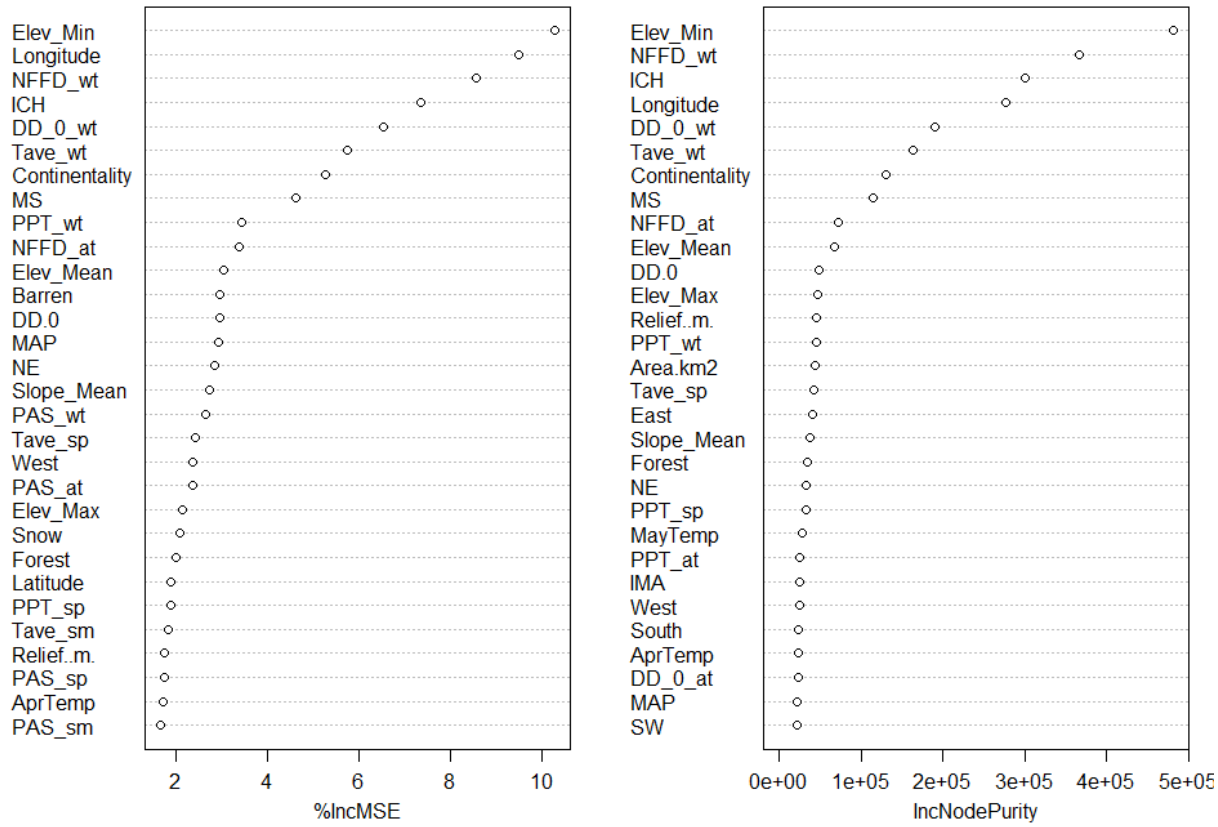

Figure 10. Eastern mountainous region, using the median SCA: Variable importance plots from a random forest regression using all physical and climatic variables. The top 30 variables are shown.

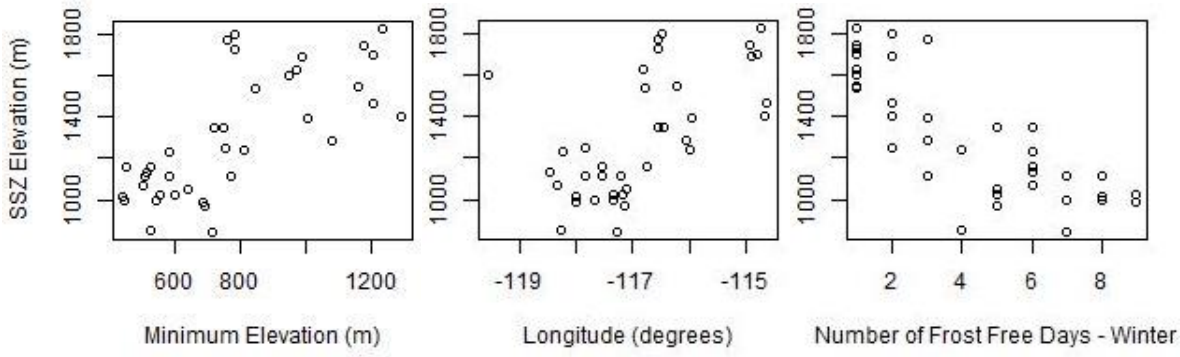

Figure 11. Eastern mountainous region, using the median SCA: Lower elevation of the SSZ plotted against the top three predictor variables identified using random forest regression.

Residuals were inspected and found to be normally distributed. There was a slight U-shaped pattern to the residuals when plotted against the predicted values (Figure 12, upper left), which indicated that a linear equation may not be the best representation of the relationship between $Elev_{medianSCA\_East}$ and one or more of the predictor variables. A similar U-shaped relationship was evident when the residuals were plotted against the number of frost-free days in the winter (NFFD_wt) (Figure 12, lower right) and in the plot of SSZ elevation versus NFFD_wt (Figure 11, right), indicating that this was the likely source of the pattern in residuals.

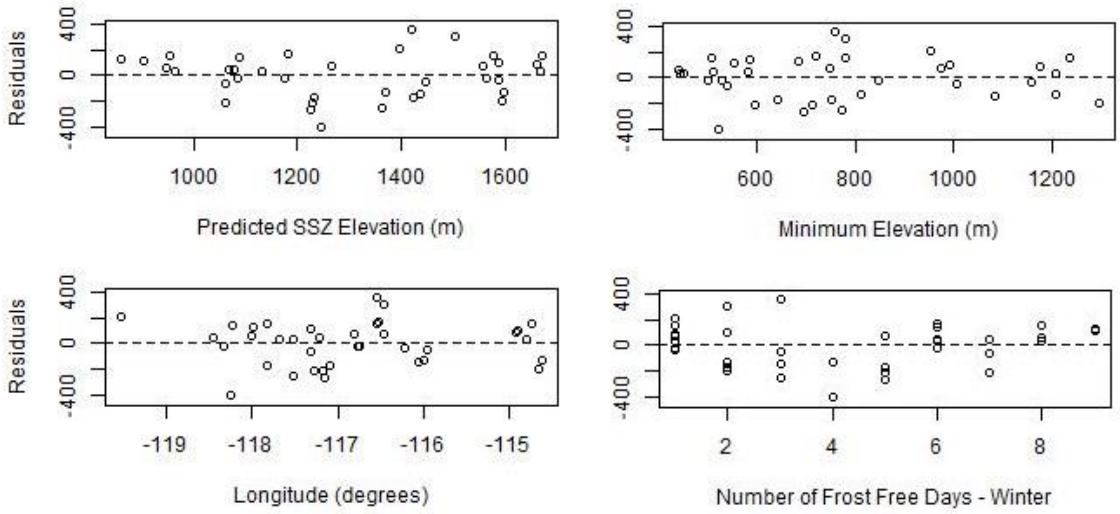

Figure 12. Eastern mountainous region, using the median SCA: Linear regression model residuals plotted against fitted values (upper left) and the independent variables.

SSZ from the Maximum SCA

Random forest regression was used to identify the most important physical and climatic variables for predicting SSZ elevation in the eastern mountainous region using the maximum SCA (n = 21, residual standard error = 173 m, variance explained = 62%). Three factors were identified whose exclusion increased the mean square error by >5%: the fractional areas in the Montane Spruce (MS) and Interior Cedar Hemlock (ICH) BEC zones, and the minimum basin elevation (Elev_Min) (Figure 13 and Figure 14). The same factors topped the list of variables that increased node purity.

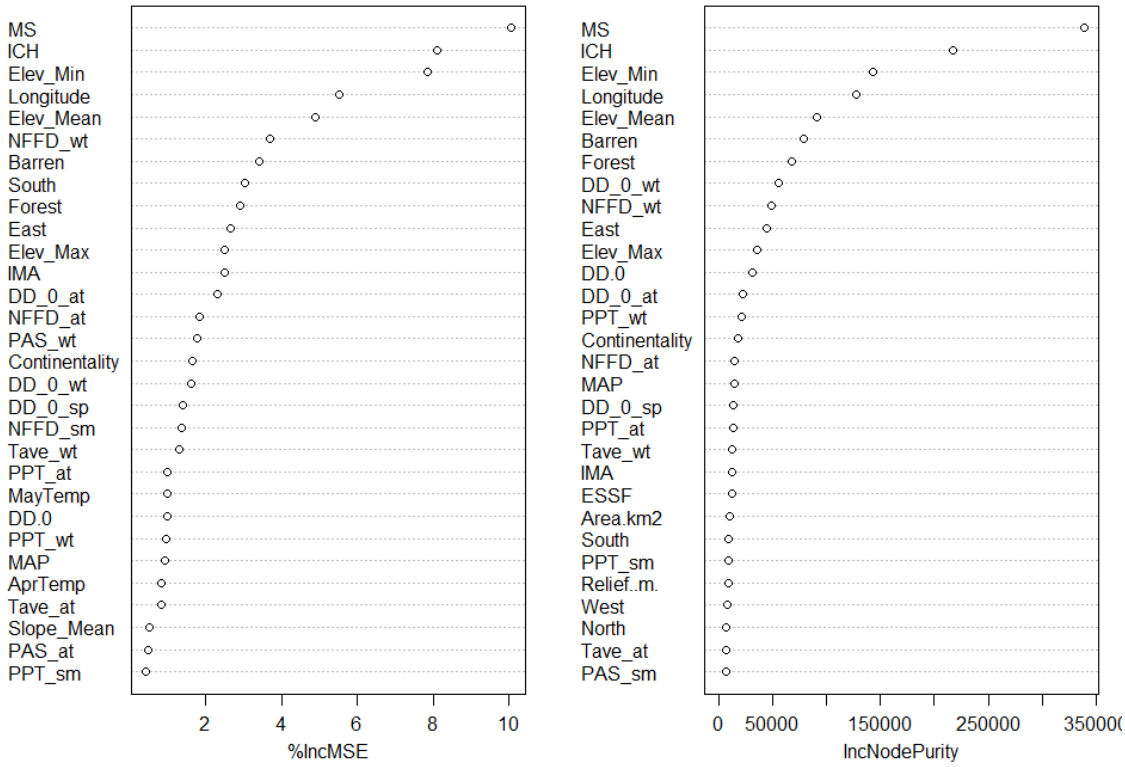

Figure 13. Eastern mountainous region, using the maximum SCA: Variable importance plots from a random forest regression using all physical and climatic variables. The top 30 variables are shown.

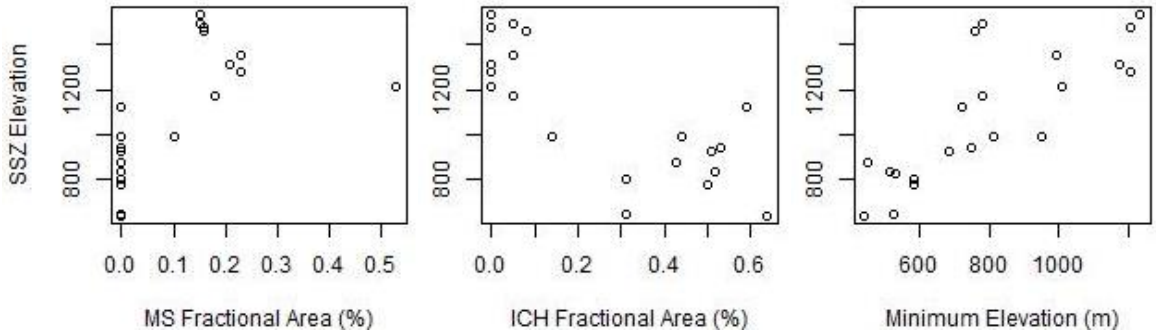

Figure 14. Eastern mountainous region, using the maximum SCA: Lower elevation of the SSZ plotted against the top three predictor variables identified using random forest regression.

The linear regression model using only the MS fractional area had an adjusted R^2 value of 36% and residual standard error of 231 m ($p<0.005$). Including the ICH and Elev_Min variables in the linear regression increased the variability explained (65%) and residual standard error (171 m) ($p<0.001$). The three-variable linear regression took the form:

$$Elev_{max\,SCA\_East} = 812.35 + 82.44MS - 495.34ICH + 0.493\ Elev\_Min$$

where $Elev_{maxSCA\_East}$ is the lower limit elevation of the SSZ estimated using the maximum SCA value for the eastern physiographic region. The residuals did not indicate bias though there was a slight U shaped pattern when the residuals were plotted against ICH (Figure 15, lower left).

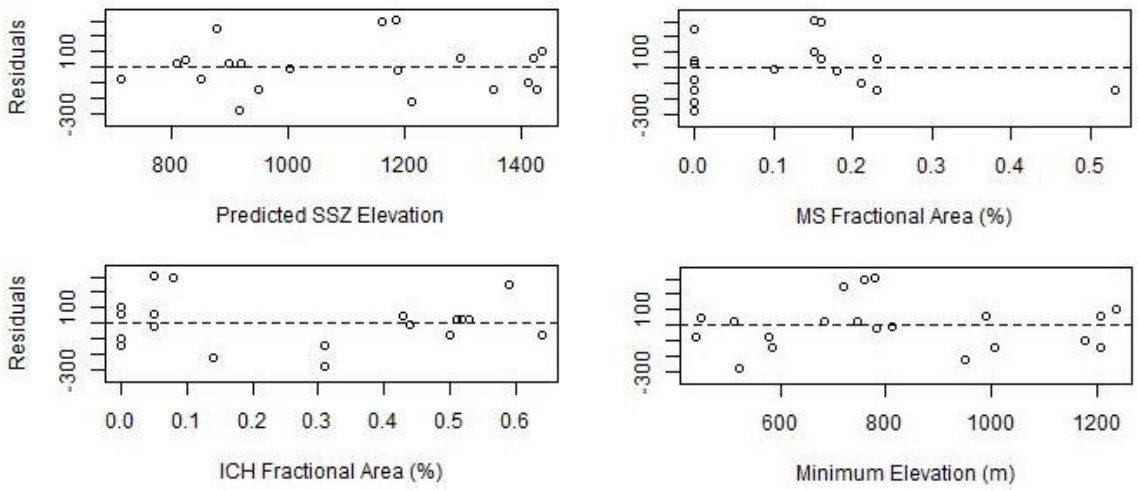

Figure 15. Eastern mountainous region, using the maximum SCA: Linear regression model residuals plotted against fitted values (upper left) and the independent variables.

3.3.2 Western Plateau Region

SSZ from the Median SCA

Random forest regression was used to identify the most important physical and climatic variables for predicting SSZ elevation in the western plateau region using the median SCA (n = 11, residual standard error = 105 m, variance explained = 14%). The low R^2 was likely due to the small sample size. Two factors were identified whose exclusion increased the mean square error by >3.5%: mean total autumn precipitation (PPT_at), and the number of frost-free days in the spring (NFFD_sp) (Figure 16 and Figure 17). These two? factors were also in the top two that increased node purity. Inclusion of two additional variables, a continentality index (Continentality) and annual degree days below 0°C (DD.0), decreased mean square error by >3% but they were not consistently at the top of the list to increase node purity (Figure 16).

Correlation analysis indicated that the mean number of frost-free days in the autumn (NFFD_at) had the strongest correlation coefficient (r = -0.83) (Figure 17). The analysis was limited to a single factor because of the small sample size, the high risk of overfitting, and there being no justification for a more complex equation.

The model fit for linear regressions using (a) the top two predictor variables from random forest regression and (b) the single variable identified using correlation analysis were similar and much better than the random forest regression results (this discrepancy was likely caused by the small sample size). The two variable regression model had an adjusted R^2 value of 66% and residual standard error of 69 m ($p<0.01$). The single variable regression using only NFFD_at had an adjusted R^2 of 65% and residual standard error of 71 m ($p<0.01$). Because the results were similar, the simpler single variable relationship is reported:

$$Elev_{median\ SCA\_West} = 2216.18 - 24.36NFFD\_at$$

where $Elev_{medianSCA\_West}$ is the lower limit elevation of the SSZ estimated using the median SCA value for the western physiographic region.

Residuals were inspected and found to be normally distributed and not biased when plotted against the three predictor variables (Figure 18).

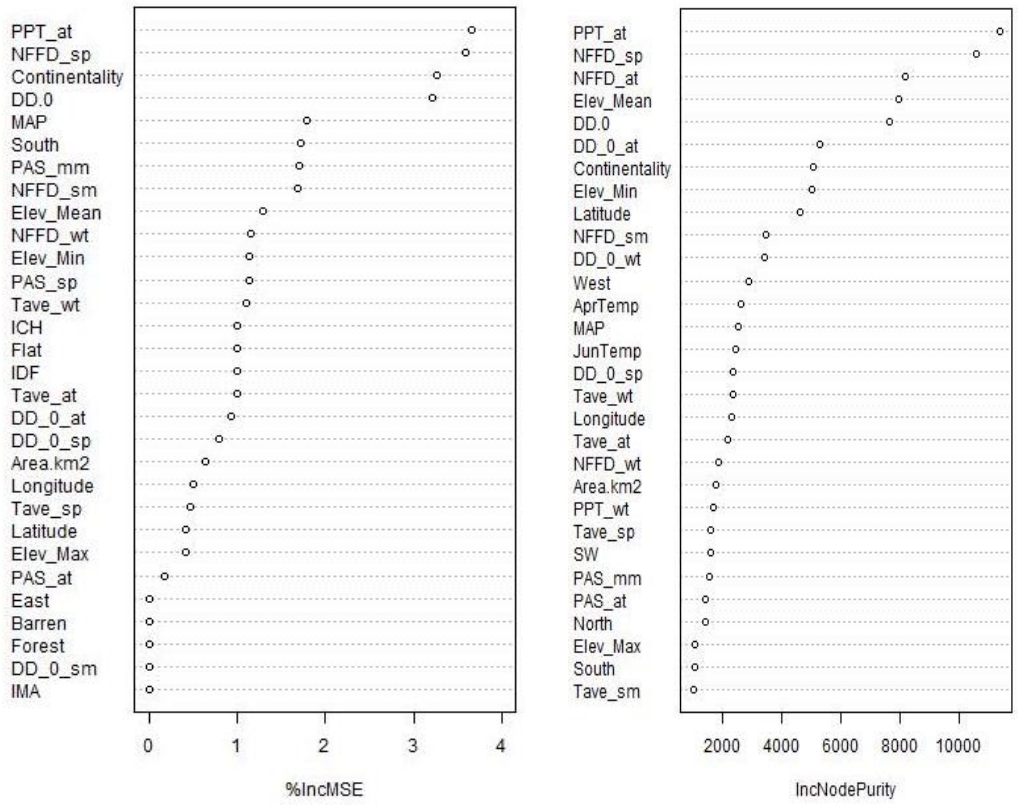

Figure 16. Western plateau region, using the median SCA: Variable importance plots from a random forest regression using all physical and climatic variables. The top 30 variables are shown.

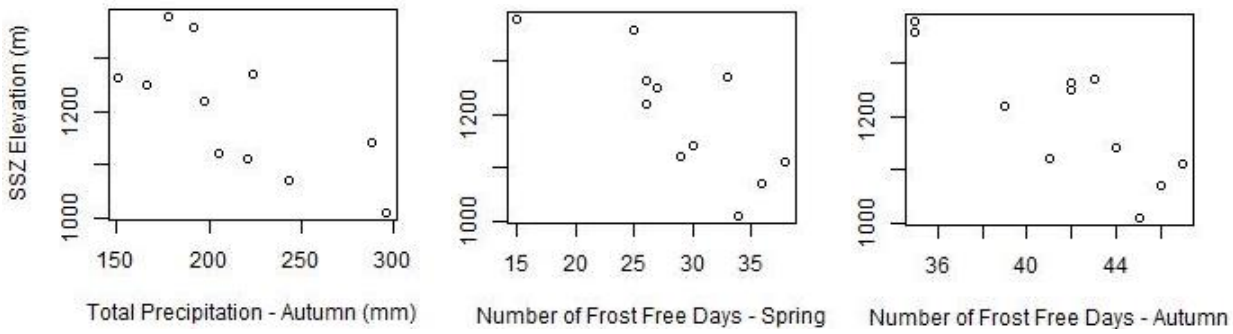

Figure 17. Western plateau region, using the median SCA: Lower elevation of the SSZ plotted against the top two predictor variables identified using random forest regression (left and centre) and the variable with the strongest correlation (right).

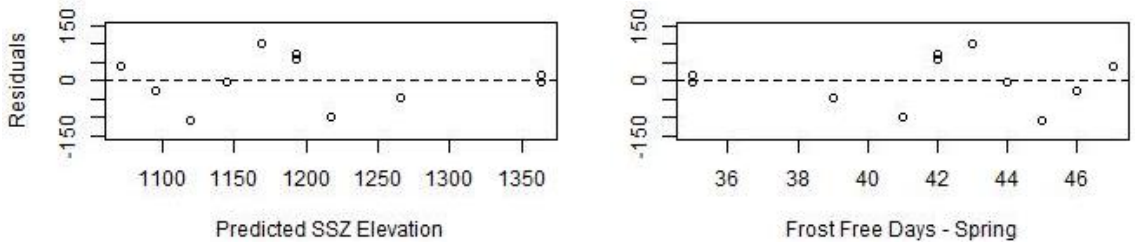

Figure 18. Western plateau region, using the median SCA: Linear regression model residuals plotted against fitted values (upper left) and the independent variable.

SSZ from the Maximum SCA

Random forest regression was used to identify the most important physical and climatic variables for predicting SSZ elevation in the western plateau region using the maximum SCA (n = 7, residual standard error = 164 m, variance explained = -32%). A negative R^2 value indicates that a regression model fits the data more poorly than a horizontal line. In this analysis, the negative result was likely due to the small sample size. Correlation analysis indicated that the mean number of frost-free days in the spring (NFFD_sp) had the strongest correlation coefficient (r = -0.89) and was used in a linear regression (Figure 19). The analysis was limited to a single factor because of the small sample size, the high risk of overfitting, and there being no justification for a more complex equation.

A linear regression using NFFD_sp had an adjusted R^2 value of 74% and residual standard error of 78 m ($p<0.01$) and had the form:

$$Elev_{maxSCA\_West} = 1555.47 - 17.58NFFD\_sp$$

where $Elev_{maxSCA\_West}$ is the lower limit elevation of the SSZ estimated using the maximum SCA value for the western plateau region. Initial assessment of the residuals indicated no bias but more points are needed to fully inspect the residuals (Figure 20).

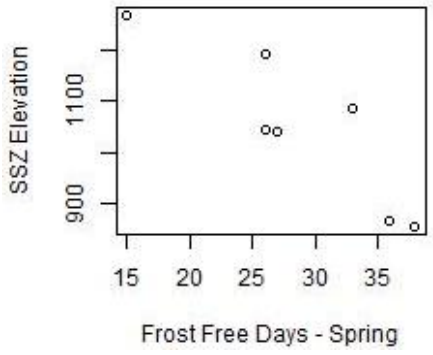

Figure 19. Western plateau region, using the maximum SCA: Lower elevation of the SSZ plotted against the top predictor variable identified using correlation analysis.

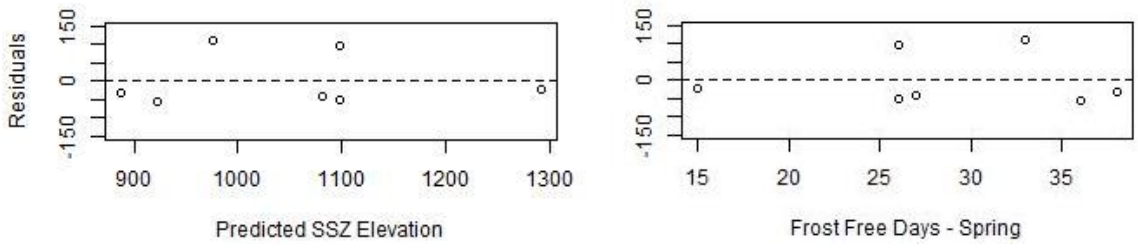

Figure 20. Western plateau region, using the maximum SCA: Linear regression model residuals plotted against fitted values (left) and the independent variable.

4. DISCUSSION

This study focussed on watersheds within the upper Columbia River basin in Canada, divided between those in the Shuswap and Okanagan Highlands and the Thompson Plateau physiographic regions in the west, and those in the Columbia Mountains and Rocky Mountains in the east (Moore and McKendry 1996; Church and Ryder 2010). Very different sets of predictors were found between the two regions, and these relationships are explored in this section.

In the eastern mountainous region, there was a positive correlation between the SSZ elevation (from both the median and maximum SCA values) and basin minimum elevation, indicating the importance of elevation in snowfall and melt processes. Longitude and the fractional areas in the ICH and MS biogeoclimatic ecosystem classification zones were also important predictors and are variables that integrate spatial patterns in other conditions and processes, such as climate, continentality and elevation. Longitude can represent distance from the Pacific Ocean, a dominant source of precipitable water in southeastern B.C. However, in the study region this general pattern of available water is overlain by orographic precipitation patterns of drier and wetter belts associated with multiple mountain ranges. Longitude also integrates a general rise in elevation moving from west to east. Larger glaciers occur in the northeastern portion of the region and are mostly absent in the southwest. While longitude itself does not determine snow accumulation and melt processes, it may be a proxy for other variables in the regressions.

The ICH and MS BEC zones both occur in lower to mid-elevation areas in the upper Columbia River basin, intermediate between Engelmann Spruce – Subalpine Fir (ESSF) at higher elevations and Interior Douglas Fir (IDF) at lower elevations. The MS BEC zone, characterised as having cold winters, is more prevalent in the Rocky Mountains while the ICH, characterised by cool and wet winters, is more common in the Columbia Mountains. The $Elev_{maxSCA\_East}$ was higher in watersheds with higher MS areas and lower in basins with higher ICH areas (Figure 14), which indicated that precipitation may be more important than temperature in determining the relationship between these two BEC zones on the SSZ elevation. More detailed analysis comparing SSZ elevations with subzones within the ICH and MS BEC zones could be done to clarify these relationships.

The only strictly climatic variable that emerged in the regression analysis for the eastern region was the mean number of frost-free days in the winter season determined at the basin centroid, which was negatively correlated with $Elev_{medianSCA\_East}$. The inclusion of winter NFFD was interpreted as representing the number of days when snowmelt or winter precipitation falling as rain may have occurred. The importance of the minimum watershed elevation variable became clearer when considered in combination with winter NFFD. On its own, the inclusion of minimum elevation in the regression for median SCA in the eastern region appeared spurious since the snowline should not be determined by the location of a watershed in the landscape but rather by climatic and regional/synoptic scale considerations. However, a higher value for winter NFFD at the basin centroid would indicate more mid-winter melt events at lower elevations in the watershed, the spatial extent of which may be inferred using the minimum elevation.

Climatic variables were more important in determining the SSZ elevation when using the median SCA in the western plateau region, indicating the importance of climate and weather in determining snow accumulation and melt patterns. The flatter topography in the headwater regions reduced the influence of physical characteristics such as slope and aspect. The predictor variables identified, mean autumn precipitation and the number of spring frost-free days, may be proxies for average winter duration and severity in the plateau watersheds.

Because of small sample size and poor model fit, it is difficult to interpret the regression relationship determined for SSZ elevations derived from maximum SCA. Mean elevation can provide a first estimate of this conservative representation of the SSZ, but more points are needed to evaluate the accuracy of the relationship.

The climatic variables used in this analysis were derived for artificial points based on the basin centroid and mean elevation. These values could be refined by deriving mean or median values from gridded datasets that represent the full range of values across the mapped basin areas. This could result in very different values for watersheds that are irregular in shape and may help improve the predictive power of the linear regressions.

While the drainage basins used in this analysis represented a wide range of sizes, climates and elevations, spatial representation across the upper Columbia River basin was patchy. Significant gaps in spatial coverage occurred: in the Okanagan River basin (WSC zone 08NM) where there were few systems defined as "natural" in the WSC database; in the less populated northern part of the study area (08NC); and in the Kootenay River watershed upstream of Lake Koocanusa (08NF and 08NG). All of the statistical analyses could be improved by including more watersheds. While 34 basins were analysed in the eastern mountainous region using SSZ estimated from the median SCA, this number was reduced to 19 when the maximum SCA was used to estimate the SSZ. In the western plateau region, sample sizes were only 11 and 7, respectively. To expand the number of basins used in this analysis to include regulated systems (especially in the Okanagan River basin), naturalised streamflow data could be created by correcting for water withdrawals and reservoir management. Similarly, artificial streamflow records generated by spatially distributed hydrologic models could provide a potential approach to validate the results presented in this report and/or to estimate the SSZ in ungauged basins. Finally, watersheds in similar physiographic and climatic regions, especially those adjacent to the Columbia River basin study area, could be included to increase the sample size. Until that analysis is conducted, applying the linear regressions for watersheds in the western plateau physiographic region to estimate SSZ elevations in ungauged watersheds should be done cautiously and be complemented with other sources of information.

The multi-platform methods used to produce the SNODAS data unfortunately result in limited opportunities to validate the product. However, because SNODAS combines model outputs with satellite, airborne and ground observations to estimate SWE, the level of uncertainty in the dataset is lower than for products that use only satellite- or ground-based information. Previous studies have concluded that SNODAS SWE products perform well in the western U.S. relative to passive microwave products (Gan et al. 2021), but that they tend to overestimate SWE in complex terrain, alpine areas, in deep snow and denser forest canopy, for ephemeral snow covers and with increasing distance from ground observation stations (Clow et al. 2012; Boniface et al. 2015; Hedrick et al. 2015; Bair et al. 2016; Musselman et al. 2018; Gan et al. 2021). Improvements were found through better representation of wind redistribution of snow during the winter, sublimation and subcanopy melt processes (Lv et al. 2019). In addition, SWE may be overestimated in the spring because the ground observation stations used in the modelling are located in clearings and at high elevations where there is more snow compared to adjacent forest stands (Dozier et al. 2016; Lv et al. 2019). In this analysis, the effect of SWE overestimation by SNODAS was ameliorated through use of a presence/absence mapping and the adoption of a threshold of 25 mm SWE. Further work comparing SCA from SNODAS with methods using other satellite and remotely sensed products that have different spatial resolutions would be useful to assess the accuracy of these results.

Snow covered area was determined for eleven years (2010-2020) to integrate interannual variability in snow accumulation and melt. There was at least one extreme year in the study period; regional climate

patterns resulting from the Pacific Ocean 'warm blob' off the west coast of B.C. during the 2014-15 winter snow accumulation and spring melt seasons resulted in either very early peak flow periods or very low SCA values across most of the study region. The influence of this year was mitigated by using the median SCA instead of the mean. Considering the relatively small number of years analysed, the median statistic may better represent the central tendency. In watersheds that are more hydrologically sensitive to changes in forest cover, a more conservative estimate of the SSZ may be made using the maximum SCA measured over the study period. However, given the tendency for SNODAS to overestimate SWE in mountainous topography and in the spring season, as described above, the median SCA may already be a relatively conservative estimate of the SSZ. Further work is needed to assess operational use of the median vs. maximum SCA to represent the SSZ.

The concept of the SSZ is somewhat nebulous and there are two important aspects to consider when assessing the high inherent uncertainty in estimating the SSZ. First, the SSZ is assumed to represent 'average' snow conditions, whereas interannual variability in winter and spring weather meant that the actual area contributing meltwater to peak flow was highly variable from year to year (for example, see Figure 6). Second, this study represented the lower limit of the SSZ using a single elevation. In reality, the boundary of the SSZ will not follow a single elevation contour because slope and aspect are important controls on both snow accumulation and melt patterns in hilly and mountainous terrain. For example, standard deviations of 107 – 276 m in snowline elevation have been reported in the Himalayas (Bagchi 1983). The residual standard errors from the linear regression models of 71 to 180 m fell near the range reported by Bagchi (1983), which indicated that the regression equations may provide a reasonable estimate of the SSZ in ungauged basins. It is worth re-stating that the estimated SSZ elevations should be used only as guidance for planning purposes and not as rigid thresholds across which there is a shift in hydrological processes.

Both climate variability and climate change are important considerations in studies of snow distribution and extent. SCA was determined for 11 recent years, a small sample size to use to represent an 'average' factor such as the snow sensitive zone. The median and maximum SCA values reported here represent conditions over the most recent decade, a time of climate non-stationarity, and it can be assumed that they are more relevant to modern management of forested landscapes than if the analysis was conducted using a longer time record. Regression analyses always benefit from having more data, but non-stationarity in climate signals could reduce our ability to predict the SSZ elevation. In contrast to the SCA record, the statistics used to identify the freshet and peak flow periods from the hydrographs were calculated for the period 1985 to 2014 (30 years), a period that presumably spans a wide range of synoptic climate conditions and low frequency climatic patterns such as the Pacific Decadal Oscillation (PDO) (as well as a period of increasing water withdrawals for domestic and agricultural use). Under climate change, changes in the timing and rates of snow accumulation and melt are expected to reduce the amount and persistence of snow at mid-elevations in southern B.C., which in turn will likely shrink the SSZ. The extent of the SSZ and relationships to topographic and climatic factors should therefore be updated periodically, and could also be performed using gridded projected climate data. Weather conditions during the time period used in this analysis were already impacted by climate change but regular updates should be planned to assess the impacts of extreme years and non-stationarity.

Especially relevant to climate change, the SSZ represents 'average' snow accumulation and melt conditions (i.e., radiation driven melt) not extreme melting and flooding generated by rain on snow (ROS). ROS events during the snowmelt period are infrequent but have caused extreme flooding, and are expected to become more frequent in the future (Jones and Perkins 2010; Freudiger et al. 2014; Guan et al. 2016; A.Q. Liu et al. 2016; Pomeroy et al. 2016; Jeong and Sushama 2018; Musselman et al. 2018). The literature indicates that the effects of forest harvest and disturbance on ROS-generated peak

flow is highly variable and depends on properties of the snowpack, vegetation cover and weather (Harr 1986; Marks et al. 1998, 2001; Jones 2000; Jones and Perkins 2010; Garvelmann et al. 2014, 2015; Wayand et al. 2015; Pomeroy et al. 2016; Würzer et al. 2016; Würzer and Jonas 2018). Further research and modelling are required to better understand the role of forested landscape disturbance and management on ROS-driven peak flows.

5. CONCLUSION

The potential use of linear regressions to estimate the SSZ elevation in ungauged basins of the upper Columbia River basin is an incremental but important step forward in forested landscape management. SSZ information can be used by specialists to plan forest harvest activities in ways that reduce the potential for snowmelt synchronisation across elevation bands in mountainous landscapes and resultant increases in peak flow. Forest resource management that considers impacts on snow accumulation and melt processes may be customised to the climate, topography, spatial variability and forest disturbance patterns found in each catchment (Zhang and Wei 2014). Specialists can balance economic or wildfire risk reduction demands with flooding risks through consideration of differences in snow accumulation and melt with slope and aspect within the SSZ of a watershed. The SSZ information can also be used by land and resource managers when considering the cumulative effects of multiple natural and anthropogenic forest disturbances on peak flow (Yu and Alila 2019). Because of inherent ambiguity in the concept of the SSZ and its representation using a single elevation threshold, the SSZ lower limit elevations should be used only as guidance for planning purposes, not as rigid thresholds that mark a change in hydrological conditions or processes.

The objectives of this study were to estimate the SSZ for gauged watersheds in two physiographic regions within the upper Columbia River basin in Canada, and to use the results to develop regression models that use key topographic and climatic variables to predict the lower limit of the SSZ in ungauged basins. The 57 selected watersheds were grouped based on their location within the western Shuswap and Okanagan Highlands and the Thompson Plateau physiographic region, or the eastern Columbia Mountains and Rocky Mountains physiographic region (Moore and McKendry 1996; Church and Ryder 2010). The analysis indicated that the H60 elevation was not a conservative approach to estimating the SSZ in most of the study basins. The SSZ was estimated using median and maximum SCA values for the 2010-2020 period, where the maximum value may provide a more conservative estimate in hydrologically sensitive watersheds. These estimates were used in random forest regressions and correlation analyses to identify the most important predictors from a list of 48 physical and climatic variables that described each basin. For each of the western plateau and eastern mountainous physiographic regions, these predictor variables were then used to derive linear regression equations to estimate SSZ elevations using both the median and the maximum SCAs. The linear regression equations explained 65-74% of the variability in the SSZ elevations, with residual standard errors of 71 to 78 m in the western plateau and 171 to 174 m in the eastern mountainous physiographic regions. Further work is needed to validate the SSZ results using remote sensing products or spatially distributed hydrologic models. Modelling could also provide an indication of how much climate change may impact the SSZ in coming decades.

REFERENCES

Arsenault, R.; F. Brissette; J.L. Martel; M. Troin; G. Lévesque; J. Davidson-Chaput; M. Castañeda Gonzalez; A. Ameli; A. Poulin. 2020. A comprehensive, multisource database for hydrometeorological modeling of 14,425 North American watersheds. Scientific Data. 7: 243. https://doi.org/10.6084/m9.figshare.12600281.

Artan, G.A.; J.P. Verdin; R. Lietzow. 2013. Large scale snow water equivalent status monitoring: Comparison of different snow water products in the upper Colorado basin. Hydrology and Earth Systems Sciences. 17: 5127-5139. https://doi.org/10.5194/hess-17-5127-2013.

Bagchi, A.K. 1983. Generation of the snowline. Photogrammetric Engineering and Remote Sensing. 49(12): 1679-1689.

Bair, E.H.; R. Davis; K. Rittger; J. Dozier. 2013. Operational SWE forecasts using a hybrid approach. Proceedings of the International Snow Science Workshop (ISSW 2013), Grenoble Chamonix-Mont-Blanc, France. 7-11 October 2013. Pp. 1293-1297.

Bair, E.H.; K. Rittger; R.E. Davis; T.H. Painter; J. Dozier. 2016. Validating reconstruction of snow water equivalent in California's Sierra Nevada using measurements from the NASA Airborne Snow Observatory. Water Resources Research. https://doi.org/10.1002/2016WR018704.

Barrett, A.P. 2003. National Operational Hydrologic Remote Sensing Center SNOw Data Assimilation System (SNODAS) products at NSIDC. NSIDC Special Report 11. National Snow and Ice Data Center: Boulder, Colorado. https://nsidc.org/sites/default/files/nsidc_special_report_11.pdf.

B.C. Ministry of Forests. 2001. Watershed assessment procedure guidebook. 2nd edition. Forest Practices Branch, Ministry of Forests. Victoria, B.C. Forest Practices Code of British Columbia Guidebook.

B.C. River Forecast Centre. 2015. Snow survey and water supply bulletins. British Columbia Ministry of Forests, Lands and Natural Resources.

Boniface, K.; J.J. Braun; J.L. McCreight; F.G. Nievinski. 2015. Comparison of Snow Data Assimilation System with GPS reflectometry snow depth in the western United States. Hydrological Processes. 29: 2425-2437. https://doi.org/10.1002/hyp.10346.

Boon, S. 2012. Snow accumulation following forest disturbance. Ecohydrology. 5: 279-285. https://doi.org/10.1002/eco.212.

Brimley, B; J.-F. Cantin; D. Harvey; M. Kowalchuk; P. Marsh; T. Ouarda; B. Phinney; P. Pilon; M. Renouf; B. Tassone; R. Wedel; T. Yuzyk. 1999. Establishment of the Reference Hydrometric Basin Network (RHBN) for Canada. Environment Canada.

Broxton, P.D.; N. Dawson; X. Zeng. 2016. Linking snowfall and snow accumulation to generate spatial maps of SWE and snow depth. Earth and Space Science. 3:246-256. https://doi.org/10.1002/2016EA000174.

Clow, D.W.; L. Nanus; K.L. Verdin; J. Schmidt. 2012. Evaluation of SNODAS snow depth and snow water equivalent estimates for Colorado Rocky Mountains, USA. Hydrological Processes. 26: 2583-2591. https://doi.org/10.1002/hyp.9385.

Dobson, D. 2013. Penticton Creek source assessment. Report prepared for the City of Penticton by Urban Systems. https://www.obwb.ca/newsite/wp-content/uploads/2013-11-19-Penticton-Creek-Source-Assessment-Report_FINAL.rev_.pdf.

Dobson Engineering Ltd. 2003a. Extent of snow cover during the 2002 spring freshet for the Mission Creek watershed (Second year of snowline data). Unpublished report. https://a100.gov.bc.ca/pub/acat/public/viewReport.do?reportId=2969.

Dobson Engineering Ltd. 2003b. Extent of snow cover during the 2002 spring freshet for the Peachland Creek watershed (Second year of snowline data). Unpublished report. https://a100.gov.bc.ca/pub/acat/public/viewReport.do?reportId=2970.

Dobson Engineering Ltd. 2003c. Extent of snow cover during the 2002 spring freshet for the Trout Creek watershed (Second year of snowline data). Unpublished report. https://a100.gov.bc.ca/pub/acat/public/viewReport.do?reportId=2971.

Dobson Engineering Ltd. 2004a. 2004 snowline survey in selected watersheds of the Central and South Okanagan (Year 2 of 5). Report prepared for Weyerhauser Company Limited. https://a100.gov.bc.ca/pub/acat/public/viewReport.do?reportId=2132.

Dobson Engineering Ltd. 2004b. Chase Creek hydrologic assessment: Impact of Mountain Pine Beetle infestations on peak flow (including application of the Ministry of Forest's Extension Note 67). Report prepared for Riverside Forest Products Ltd. And Tolko Industries Ltd. https://www.for.gov.bc.ca/hfd/library/FIA/2005/FIA2005MR024-1.pdf.

Dobson Engineering Ltd. 2004c. Snowline data for the Trout Creek watershed: Extent of snow cover during the 2004 spring freshet. Report prepared for Riverside Forest Products Limited and Gorman Bros. Lumber Limited. https://a100.gov.bc.ca/pub/acat/public/viewReport.do?reportId=2905.

Dobson Engineering Ltd. 2005a. Snowline data for the Mission Creek watershed: Extent of snow cover during the 2004 spring freshet. Report prepared for Riverside Forest Products Limited and Gorman Bros. Lumber Limited. https://a100.gov.bc.ca/pub/acat/public/viewReport.do?reportId=2906.

Dobson Engineering Ltd. 2005b. Snowline data for the Peachland Creek watershed: Extent of snow cover during the 2004 spring freshet. Report prepared for Riverside Forest Products Limited and Gorman Bros. Lumber Limited. https://a100.gov.bc.ca/pub/acat/public/viewReport.do?reportId=2903.

Dobson Engineering Ltd. 2005c. Snowline data for the Shingle Creek watershed: Extent of snow cover during the 2004 spring freshet. Report prepared for Gorman Bros. Lumber Limited and Riverside Forest Products Limited. https://a100.gov.bc.ca/pub/acat/public/viewReport.do?reportId=2904.

Dobson Engineering Ltd. 2005d. Snowline data for the Trout Creek watershed: Extent of snow cover during the 2004 spring freshet. Report prepared for Riverside Forest Products Limited and Gorman Bros. Lumber Limited.

Dozier, J.; E.H. Bair; R.E. Davis. 2016. Estimating the spatial distribution of snow water equivalent in the world's mountains. WIREs Water. 3: 461-474. https://doi.org/10.1002/wat2.1140.

Driscoll, J.M.; L.E. Hay; A.R. Bock. 2017. Spatiotemporal variability of snow depletion curves derived from SNODAS for the coterminous United States, 2004-2013. Journal of the American Water Resource Association. 53(3): 655-666. https://doi.org/10.1111/1752-1688.12520.

Freudiger, D.; I. Kohn; K. Stahl; M. Weiler. 2014. Large scale analysis of changing frequencies of rain-on-snow events with flood-generation potential. Hydrology and Earth System Sciences. 18(7): 2695-2709. https://doi.org/10.5194/hess-18-2695-2014.

Gan, Y.; Y. Zhang; C. Kongoli; C. Grassotti; Y. Liu; Y.K. Lee; D.J. Seo. 2021. Evaluation and blending of ATMS and AMSR2 snow water equivalent retrievals over the conterminous United States. Remote Sensing of Environment. 254:112280. https://doi.org/10.1016/j.rse.2020.112280.

Gartska, W.U.; L.D. Love; B.C. Goodell; F.A. Bertle. 1958. Factors affecting snowmelt and streamflow: A report on the 1946-53 cooperative snow investigations at the Fraser Experimental Forest, Fraser, Colorado. U.S. Department of the Interior, Bureau of Land Management and U.S. Department of Agriculture, Forest Service.

Garvelmann, J.; S. Pohl; M. Weiler. 2014. Variability of observed energy fluxes during rain-on-snow and clear sky snowmelt in a midlatitude mountain environment. Journal of Hydrometeorology. 15: 1220-1237. https://doi.org/10.1175/JHM-D-13-0187.1.

Garvelmann, J.; S. Pohl; M. Weiler. 2015. Spatio-temporal controls of snowmelt and runoff generation during rain-on-snow events in a mid-latitude mountain catchment. Hydrological Processes. 29: 3649-3664. https://doi.org/10.1002/hyp.10460.

Gayton, D.; D. Wrangler. 2003. A proud tradition: History of the Nelson Forest Region 1897-2003. British Columbia Ministry of Forests, online at: https://www.for.gov.bc.ca/rsi/proudtraditionpart2.pdf.

Gluns, D.R. 2001. Snowline patterns during the melt season: Evaluation of the H60 concept. In Watershed Assessment in the Southern Interior of British Columbia: Workshop Proceedings. D.A.A. Toews and S. Chatwin (eds.). 9-10 March 2000: Penticton, B.C. Pp. 68-80. https://www.for.gov.bc.ca/hfd/pubs/docs/wp/wp57/Wp57-02.pdf.

Guan, B.; N.P. Molotch; D.E. Waliser; E.J. Fetzer; P.J. Neiman. 2013a. The 2010/2011 snow season in California's Sierra Nevada: Role of atmospheric rivers and modes of large-scale variability. Water Resources Research. 49: 6731-6743. https://doi.org/10.1002/wrcr.20537.

Guan, B.; N.P. Molotch; D.E. Waliser; S.M. Jepsen; T.H. Painter; J. Dozier. 2013b. Snow water equivalent in the Sierra Nevada: Blending snow sensor observations with snowmelt model simulations. Water Resources Research. 49: 5029-5043. https://doi.org/10.1002/wrcr.20387.

Guan, B.; D.E. Waliser; F.M. Ralph; E.J. Fetzer; P.J. Neiman. 2016. Hydrometeorological characteristics of rain-on-snow events associated with atmospheric rivers. Geophysical Research Letters. 43: 2964-2973. https://doi.org/10.1002/2016GL067978.

Hammond, J.C.; B.J. Fleming. 2021. Evaluating low flow patterns, drivers and trends in the Delaware River Basin. Journal of Hydrology. 598: 126246. https://doi.org/10.1016/j.jhydrol.2021.126246.

Hammond, J.C.; F.A. Saavedra; S.K. Kampf. 2018. How does snow persistence relate to annual streamflow in mountain watersheds of the western U.S. with wet maritime and dry continental climates? Water Resources Research. 54. https://doi.org/10.1002/2017WR021899.

Harr, R.D. 1986. Effects of clearcutting on rain-on-snow runoff in western Oregon: A new look at old studies. Water Resources Research. 22(7): 1095-1100. https://doi.org/10.1029/WR022i007p01095.

Hedrick, A.; H.-P. Marshall; A. Winstral; K. Elder; S. Yueh; D. Cline. 2015. Independent evaluation of the SNODAS snow depth product using regional-scale lidar-derived measurements. The Cryosphere. 9: 13-23. https://doi.org/10.5194/tc-9-13-2015.

Jeong, D.I.; L. Sushama. 2018. Rain-on-snow events over North America based on two Canadian regional climate models. Climate Dynamics. 50: 303-316. https://doi.org/10.1007/s00382-017-3609-x.

Jones, J.A. 2000. Hydrologic processes and peak discharge response to forest removal, regrowth, and roads in 10 small experimental basins, western Cascades, Oregon. Water Resources Research. 36(9): 2621-2642. https://doi.org/10.1029/2000WR900105.

Jones, J.A.; R.M. Perkins. 2010. Extreme flood sensitivity to snow and forest harvest, western Cascades, Oregon, United States. Water Resources Research. 46. https://doi.org/10.1029/2009WR008632.

Jost, G.; M. Weiler; D.R. Gluns; Y. Alila. 2007. The influence of forest and topography on snow accumulation and melt at the watershed-scale. Journal of Hydrology. 347: 101-115. https://doi.org/10.1016/j.jhydrol.2007.09.006.

Keum, J.; P. Coulibaly; T. Razavi; D. Tapsoba; A. Gobena; F. Weber; A. Pietroniro. 2018. Application of SNODAS and hydrologic models to enhance entropy-based snow monitoring network design. Journal of Hydrology. 561: 688-701. https://doi.org/10.1016/j.jhydrol.2018.04.037.

Lea, J. 2007. The NOHRSC SNODAS snow water equivalent determination on Mount St. Helens, Washington. Proceedings of the Western Snow Conference. Pp. 175-178. https://westernsnowconference.org/sites/westernsnowconference.org/PDFs/2007Lea.pdf.

Liaw, A.; Wiener, M. 2002. "Classification and Regression by randomForest." R News 2(3): 18-22. https://CRAN.R-project.org/doc/Rnews/.

Liu, A.Q.; C. Mooney; K. Szeto; J.M. Thériault; B. Kochtubajda; R.E. Stewart; S. Boodoo; R. Goodson; Y. Li; J. Pomeroy. 2016. The June 2013 Alberta catastrophic flooding event: Part 1 – Climatological aspects and hydrometorological features. Hydrological Processes. 30: 4899-4916. https://doi.org/10.1002/hyp.10906.

Liu, X.; L. Jiang; G. Wang; S. Hao. 2016. Improvement of long-term snow depth product accuracy from passive microwave satellite observations: A case study with SNODAS data. 2016 IEEE International Geoscience and Remote Sensing Symposium (IGARSS). Pp. 4876-4879. DOI: 10.1109/IGARSS.2016.7730272.

Liu, X.; L. Jiang; G. Wang; S. Wang. 2019. Deriving long-term snow depth datasets from passive microwave observations – A case study in the United States. 2019 IEEE International Geoscience and Remote Sensing Symposium (IGARSS). Pp. 4117-4120. DOI: 10.1109/IGARSS.2019.8899112.

Lv, Z.; J.W. Pomeroy; X. Fang. 2019. Evaluation of SNODAS snow water equivalent in Western Canada and assimilation into a cold region hydrological model. Water Resources Research. 55: 11166-11187. https://doi.org/10.1029/2019WR025333.

Marks, D.; J. Kimball; D. Tingey; T. Link. 1998. The sensitivity of snowmelt processes to climate conditions and forest cover during rain-on-snow: A case study of the 1996 Pacific Northwest flood. Hydrological Processes. 12: 1569-1587. https://doi.org/10.1002/(SICI)1099-1085(199808/09)12:10/11<1569::AID-HYP682>3.0.CO;2-L.

Marks, D.; T. Link; A. Winstral; D. Garen. 2001. Simulating snowmelt processes during rain-on-snow over a semi-arid mountain basin. Annals of Glaciology. 32: 195-202. https://doi.org/10.3189/172756401781819751.

Massmann, C. 2019. Modelling snowmelt in ungauged catchments. Water. 11:301. https://doi.org/10.3390/w11020301.

Matos, A.; Dilts, T.E. 2019. Hypsometric Integral Toolbox for ArcGIS. University of Nevada Reno. Available at https://www.arcgis.com/home/item.html?id=23a2dd9d127f41c195628457187d4a54.

Moore, R.D.; I.G. McKendry. 1996. Spring snowpack anomaly patterns and winter climatic variability, British Columbia, Canada. Water Resources Research. 32 (3): 623-632. https://doi.org/10.1029/95WR03640.

Musselman, K.N.; F. Lehner; K. Ikeda; M.P. Clark; A.F. Prein; C. Liu; M. Barlage; R. Rasmussen. 2018. Projected increases and shifts in rain-on-snow flood risk over western North America. Nature Climate Change. 8: 808-812. https://doi.org/10.1038/s41558-018-0236-4.

National Operational Hydrologic Remote Sensing Center (NOHRSC). 2004. Snow Data Assimilation System (SNODAS) Data Products at NSIDC, Version 1. 2010-2020 subset for southern British Columbia. Boulder, Colorado USA. NSIDC: National Snow and Ice Data Center. https://doi.org/10.7265/N5TB14TC.

Neumann, N. 2022. Assessing the “snow sensitive zone” at multiple scales in the Kettle River watershed, southern British Columbia. Water Science Series WSS2022-02. Province of British Columbia: Victoria, B.C. https://a100.gov.bc.ca/pub/acat/public/viewReport.do?reportId=59526.

Pike, R.G.; D.J. Wilford. 2013. Desktop watershed characterization methods for British Columbia. Province of British Columbia: Victoria B.C. Technical Report 079. https://www.for.gov.bc.ca/hfd/pubs/Docs/Tr/TR079.pdf.

Pomeroy, J.W.; R.E. Stewart; P.H. Whitfield. 2015. The 2013 flood event in the South Saskatchewan and Elk River basins: Causes, assessment and damages. Canadian Water Resources Journal. https://doi.org/10.1080/07011784.2015.1089190.

Pomeroy, J.W.; X. Fang; D.G. Marks. 2016. The cold rain-on-snow event of June 2013 in the Canadian Rockies – Characteristics and diagnosis. Hydrological Processes. 30: 2899-2914. https://doi.org/10.1002/hyp.10905.

R Core Team. 2022. R: A language and environment for statistical computing. R Foundation for Statistical Computing: Vienna, Austria. http://www.R-project.org.

Schneiderman, E.M.; A.H. Matonse; M.S. Zion; D.G. Lounsbury; R. Mukundan; S.M. Pradhanang; D.C. Pierson. 2013. Comparison of approaches for snowpack estimation in New York City watersheds. Hydrological Processes. 27: 3050-3060. https://doi.org/10.1002/hyp.9868.

Siren, A.P.K.; M. Somos-Valenuela; C. Callahan; J.R. Kilborn; T. Duclos; C. Tragert; T.L. Morelli. 2018. Looking beyond wildlife: Using remote cameras to evaluate accuracy of gridded snow data. Remote Sensing in Ecology and Conservation. 4(4): 375-386. https://doi.org/10.1002/rse2.85.

Smith, R.S.; R.A. Scherer; D.A. Dobson. 2008. Snow cover extent during spring snowmelt in the south-central interior of British Columbia. B.C. Journal of Ecosystems and Management. 9(1): 57-70. https://doi.org/10.22230/jem.2008v9n1a386.

Tedesco, M.; P.S. Narvekar. 2010. Assessment of the NASA AMSR-E SWE product. IEEE Journal of Selected Topics in Applied Earth Observations and Remote Sensing. 3(1): 141-159. DOI: 10.1109/JSTARS.2010.2040462.

Tennant, C.J.; B.T. Crosby; S.E. Godsey. 2014. Elevation-dependent responses of streamflow to climate warming. Hydrological Processes. https://doi.org/10.1002/hyp.10203.

Teti, P. 2003. Relations between peak snow accumulation and canopy density. The Forestry Chronicle. 79(2): 307-312. https://pubs.cif-ifc.org/doi/pdf/10.5558/tfc79307-2.

Varhola, A.; N.S. Coops; M. Weiler; R.D. Moore. 2010. Forest canopy effects on snow accumulation and ablation: An integrative review of empirical results. Journal of Hydrology. 392: 219-233. https://doi.org/10.1016/j.jhydrol.2010.08.009.

Vuyovich, C.M.; J.M. Jacobs; S.F. Daly. 2014. Comparison of passive microwave and modeled estimates of total watershed SWE in the continental United States. Water Resources Research. 50: 9088-9102. https://doi.org/10.1002/2013WR014734.

Wang, T.; A. Hamann; D. Spittlehouse; C. Carroll. 2016. Locally downscaled and spatially customizable climate data for historical and future periods for North America. PloS one. 11(6): e0156720. https://doi.org/10.1371/journal.pone.0156720.

Wayand, N.E.; J.D. Lundquist; M.P. Clark. 2015. Modeling the influence of hypsometry, vegetation, and storm energy on snowmelt contributions to basins during rain-on-snow floods. Water Resources Research. https://doi.org/10.1002/2014WR016576.

H. Wickham. ggplot2: Elegant Graphics for Data Analysis. Springer-Verlag New York, 2016.

Winkler, R.; D. Gluns; D. Golding. 2004. Identifying snow indices for forest planning in southern British Columbia. Proceedings of the 72nd Annual Meeting of the Western Snow Conference. Pp. 53-61. https://westernsnowconference.org/node/812.

Winkler, R.; D. Spittlehouse; S. Boon; B. Zimonick. 2015. Forest disturbance effects on snow and water yield in interior British Columbia. Hydrology Research. 46(4): 521-532. https://doi.org/10.2166/nh.2014.016.

Wrzesien, M.L.; M.T. Durand; T.M. Pavelsky; I.M. Howat; S.A. Margulis; L.S. Huning. 2017. Comparison of methods to estimate snow water equivalent at the mountain range scale: A case study of the California Sierra Nevada. Journal of Hydrometeorology. 18: 1101-1119. https://doi.org/10.1175/JHM-D-16-0246.1.

Würzer, S.; T. Jonas; N. Wever; M. Lehning. 2016. Influence of initial snowpack properties on runoff formation during rain-on-snow events. Journal of Hydrometeorology. 17: 1801-1815. https://doi.org/10.1175/JHM-D-15-0181.1.

Würzer, S.; T. Jonas. 2018. Spatio-temporal aspects of snowpack runoff formation during rain on snow. Hydrological Processes. 32: 3434-3445. https://doi.org/10.1002/hyp.13240.

Yu, X.J.; Y. Alila. 2019. Nonstationary frequency pairing reveals a highly sensitive peak flow regime to harvesting across a wide range of return periods. Forest Ecology and Management. 444: 187-206. https://doi.org/10.1016/j.foreco.2019.04.008.

Zahmatkesh, Z.; D. Tapsoba; J. Leach; P. Coulibaly. 2019. Evaluation and bias correction of SNODAS snow water equivalent (SWE) for streamflow simulation in eastern Canadian basins. Hydrological Sciences Journal. 64(13): 1541-1555. https://doi.org/10.1080/02626667.2019.1660780

Zhang, M.; X. Wei. 2014. Contrasted hydrological responses to forest harvesting in two large neighbouring watersheds in snow hydrology dominant environment: Implications for forest management and future forest hydrology studies. Hydrological Processes. 28: 6183-6195. https://doi.org/10.1002/hyp.10107.

Zheng, Z.; N.P. Molotch; C.A. Oroza; M.H. Conklin; R.C. Bales. 2015. Spatial snow water equivalent estimation for mountainous areas using wireless-sensor networks and remote-sensing products. Remote Sensing of Environment. 215:44-56. https://doi.org/10.1016/j.rse.2018.05.029.